June 2020

Techno-Economic Analysis of Floating Offshore Airborne Wind Energy Systems in the Gulf of Mexico

Alexandria Savannah Leake

TECHNO-ECONOMIC ANALYSIS OF FLOATING OFFSHORE AIRBORNE WIND ENERGY SYSTEMS IN THE GULF OF MEXICO

A Thesis

Submitted to the Graduate Faculty of the
Louisiana State University and
Agricultural and Mechanical College
in partial fulfillment of the
requirements for the degree of
Master of Science

in

The Department of Environmental Sciences

by
Alexandria Savannah Leake
B.S., Louisiana State University, 2018
August 2020

Acknowledgments

I would like to express sincere gratitude to my advisor Dr. Brian Snyder for his continued patience, motivation, and advising throughout the past two years. His guidance helped me unsurface and grow my interests and ideas relating to renewable energy research, specifically airborne wind energy technology. Dr. Snyder's constant encouragement and positive demeanor significantly helped me during difficult times, while completing my coursework and thesis. I would also like to thank my two other committee members, Dr. Vince Wilson, and Dr. Paul Miller for their support and assistance. Dr. Wilson has been a mentor to me throughout my graduate assistantship as a recruiter for the College of the Coast and Environment, and has allowed me to gain important interpersonal skills. I also had the pleasure of taking his toxicology course, leading to a new-found interest in the topic. Dr. Miller reginited my fascination in atmospheric science through his assistance with my high-altitude wind resource analysis and by taking his atmospheric modelling course. The completion of my wind resource analysis would not have been possible, without his assistance and expertise. Additionally, I would like to thank the head recruiter, Tiffany Treloar, who trained and assisted me throughout my assistantship and was a pleasure to work alongside. I would also like to thank my graduate counselor, Charlotte St. Romain who believed in my abilities when I never did, and has made one of the greatest impacts on my life. I could not have asked for better mentors throughout the past two years.

I would also like to thank my loving parents and big sister for their continued emotional support throughout my time in graduate school, even from a distance. My parents are the greatest role models I could have asked for and gave my sister and I opportunities they never had in life. Also, I would like to thank my childhood friends in Georgia, my Delta Zeta sorority sisters, and

graduate school friends for their continued support as well. I would not be in this position of graduating with my Master's degree in Environmental Sciences if I did not have such a strong support system in my life.

Table of Contents

List of Tables

List of Figures

Terminology

AWE	-Airborne Wind Energy
Break-Even Point	-Point at which total cost and revenue are equal
CAPEX	-Capital Expenditures
CF	-Capacity Factor
Conventional Wind	-Traditional wind turbine with a tower, nacelle, and blades
Crane Barge	-Flat-bottomed boat used for transporting floating wind platforms
Crane Vessel	-Ship with a crane specialized in lifting heavy loads in offshore environments
Day Rate	-Cost for a single day to use a variety of vessels for installation purposes of an offshore structure
EIA	-Environmental Impact Assessment
Generator	-Includes electrical generator, control electronics, and gearbox components, that converts incoming wind energy into usable electricity
Hywind	-Floating spar buoy platform design concept created by Equinor
Kite	-Either a soft-kite resembling an actual kite or a rigid-kite resembling an aircraft wing in an AWE system
Km	-Kilometer
kV	-Kilovolt
kW	-Kilowatt
kWh	-Kilowatt/hour
LCCA	-Life Cycle Cost Assessment
LCOE	-Levelized Cost of Energy
m	-Meter
Mooring System	-System of mooring lines and anchor on the seafloor that keep a floating platform in position
mt	-Metric ton
MW	-Megawatt
NPV	-Net Present Value
OPEX	-Operational Expenditures
ROI	-Return on Investment
Semi-Submersible	-Type of floating offshore wind platform that obtains buoyancy from ballasted, watertight rafts directly below the ocean surface
Spar Buoy	-Type of floating offshore wind platform with a center of mass below sea-level
SWAY	-Floating spar platform design concept created by Inocean and is anchored to seabed with a tension-torsion leg
Tethered Rope	-Component of AWE system in place of a tower, allowing for wind harvesting to occur at much higher altitudes
Tension Leg Buoy (TLB)	-Type of floating offshore wind platform where the buoyancy is controlled by taut mooring lines

Tension Leg Platform (TLP)	-Type of floating offshore wind platform that is stabilized by the tension in the mooring system
Transmission System	-Electrical transmission system consisting of an export cable, import cable under the seabed and a substation (>15 km from shore) that transports generated offshore wind energy to shore
Wind Farm	-Commercial assemblage of wind turbines producing electricity
WindFloat	-Floating semi-submersible platform design concept developed by Principle Power Inc.

Abstract

Techno-economic analyses play an important role in determining locations for conventional wind turbine installations. This method is utilized to assess energy production potential for a new type of wind technology, known as airborne wind energy (AWE). The first objective of the present thesis was to determine overall investment potential of a utility-scale floating offshore airborne wind farm, testing five floating platform design concepts. The second objective was to determine whether the wind resources (100-1500 m) are ideal to support AWE systems in the Gulf of Mexico. Specifically, a hypothetical benchmark wind farm was developed 15 km offshore from Venice, Louisiana. The techno-economic analysis incorporated a life-cycle cost assessment (LCCA), wind resource analysis, economic feasibility cost model, and sensitivity study. The life-cycle costs of each floating offshore AWE farm concept were determined, including the estimated costs for five life phases. The phases in the LCCA include, development and consenting, production and acquisition, installation and commissioning, operation and maintenance, and decommissioning and disposal. The wind resource analysis determined the wind harvesting potential at the hypothetical wind farm site over a 41-year period (1979-2019). The mean wind speed Weibull parameters for the combined wind harvesting heights (100-1500 m) are $c = 7.28$ m/s and $k = 4.36$, indicating the site is ideal for wind farm development, when accounting for all harvesting heights. The mean wind speed Weibull parameters are $c = 7.44$ m/s and $k = 4.88$ at 500 m. These results show that ideal wind resources exist above 500 m heights in coastal Louisiana. The economic feasibility of each wind farm concept was determined through a net present value (NPV) cost model. The purpose of the sensitivity study was to demonstrate the fluctuating output variables when key cost factors were

modified. The base case NPVs for all five wind farm concepts were originally estimated, but the final conclusions for investment potential were based on mature technology costs. Based on these results, the TLB-B wind farm has investment potential, due to the concept's positive NPV. The other four wind farm concepts, TLB-X3, Hywind, WindFloat, and SWAY produced negative NPVs and are not economically feasible.

Chapter 1. Introduction

Over the past few decades, a new technology for producing electricity known as airborne wind energy (AWE) began development. These systems incorporate a flying tethered kite or aircraft to access winds blowing at currently inaccessible altitudes by conventional wind turbines. Research began in the 1970s, with Dr. Miles Loyd pioneering the concept of AWE, and there has been a large increase in development within the last decade by several companies. The increased interest in this novel renewable energy is due to the invention of drone technology, making AWE an attainable energy solution. Different prototypes have been created thus far across the world and have reached early experimental stages.

Recently, there has been a sharp increase in renewable energy systems, particularly wind energy generators. Unfortunately, there may be a decrease in conventional wind system growth soon due to saturation of windy onshore locations that are optimal for installation. This has led to research on improvement of power capacity per unit of land area through alternative wind technology with high-length blades, increased swept area, and high-height turbine axes that reach stronger winds with increased altitudes.

The potential for offshore wind energy installations has been increasingly studied since the early 2000s, since wind resources are typically greater farther from the coast compared to those on land. The growth rate potential of offshore wind is promising, due to the constant and reliable winds. AWE systems aim to capture wind energy at much higher altitudes than is possible with conventional wind turbines at a lower cost (9).

The concept that wind energy in the atmosphere could theoretically power the world is still up for scientific debate. Alternatively, extraction of large-scale energy effects on the overall

resource and vertical energy exchange between wind layers remains uncertain. Many researched studies on this concept rely on conventional wind turbines, which only account for surface-level energy extraction. AWE systems are underrepresented when considering the feasibility of wind energy powering the entire world (5).

This thesis provides a techno-economic analysis of different technologies developed in the AWE category of renewable energy and five floating offshore platform concepts. The AWE technology that is further along in development and has been tested in real scenarios is analyzed. Also, the practicality of these systems being constructed and actively used in an offshore floating AWE farm in the Gulf of Mexico is studied.

Furthermore, this work investigates the financial payback period of five floating offshore AWE farm concepts at commercial scale, through a net present value (NPV) cost model. A life-cycle cost assessment (LCCA) approach is utilized, with multiple life phases evaluated including, development and consenting, production and acquisition, installation and commissioning, operation and maintenance, and decommissioning and disposal. The LCCA is based on a generic 2 MW AWE system and its incorporation with five floating offshore wind platform concepts. The techno-economic analysis involves a high-altitude wind resource analysis, economic feasibility cost model, and sensitivity study of all wind farm concepts. Each concept was tested for potential project investment at a hypothetical wind farm site with a total capacity of 500 MW, 15 kilometers (km) off the coast of Venice, Louisiana. Specifically, a generalized AWE lift-mode system, also referred to as a pumping-kite, is implemented and evaluated with the five floating platform concepts. Information from this study can assist decision-makers in the economic, political, and public sectors when determining the future

support of AWE system technology in an offshore environment as a probable renewable energy source.

Chapter 2. Literature Review

2.1. Airborne Wind Energy (AWE)

Airborne wind energy has the potential to generate electricity in locations where wind speeds are considered unsuitable for conventional wind turbines. While conventional turbines generate wind energy at an average hub height of 100 m, AWE is designed to harvest wind energy at varying altitudes. Most locations on Earth have larger power production capabilities with increasing altitude (4). For the purpose of this thesis, the harvesting potential of wind in the Gulf of Mexico was analyzed between 100-1500 m in height at a specific offshore site to study this concept.

There are many potential advantages to AWE. An advantage of AWE compared to conventional wind is the tower-less design, incorporating a tethered rope. This allows an AWE system to alter its flight path to different altitudes to capture the strongest winds. The capacity factor of an AWE system is higher than a conventional wind turbine at onshore and offshore locations, due to temporally steady and less chaotic winds. AWE systems use about 90% less materials than conventional wind turbines because of their tower-less design and smaller components, such as the foundation. This leads to AWE having lower electricity generation costs compared to conventional wind, because of their cheaper and lighter materials. Also, their visual and acoustic impacts are minimal since they operate at higher altitudes (4). Utility-scale AWE systems are ideal for hurricane prone areas such as the Gulf of Mexico. They can be easily towed into port or safely put in their stationary position.

2.1.1. Airborne Wind Energy System Components

There are many components that make up an AWE system. There are five general component categories with different functions, that allow an AWE system to take flight and convert high-altitude wind energy into usable electricity. An AWE system is composed of wind capturing, system control, structural, mechanical power conversion, and electrical power conversion components. The wind capturing components consist of a wing/kite and a bridle line system, while the system control consists of the kite control unit (KCU) and multiple sensors. The structural components involve the tethered rope and the launching and landing system, and the mechanical components incorporate a drum and generator. The electrical power conversion components include a battery, inverter, and transformer. All aspects incorporated into an AWE system are displayed in Figure 1.

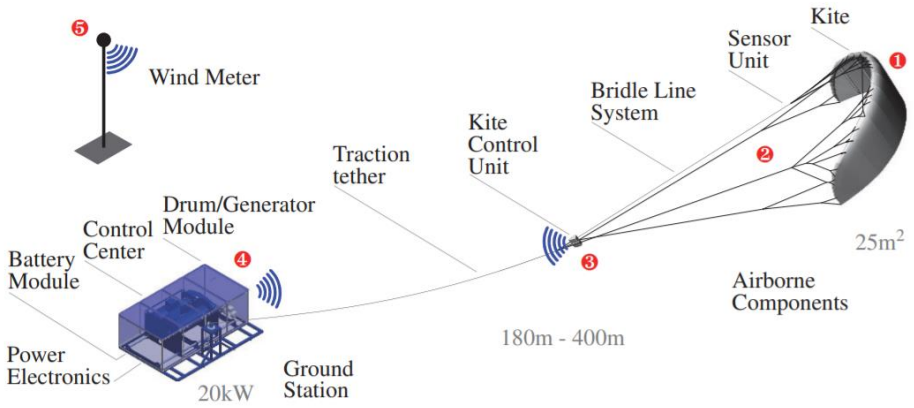

Figure 1. Generalized AWE system made up of five different component categories including, (1) wind capturing components, (2) system control components, (3) structural components, (4) mechanical power conversion components, and (5) electrical power conversion components (38).

The kite in an AWE system can either be categorized as rigid or soft. A rigid kite resembles an aircraft wing and a soft kite resembles an actual kite. The bridle line system connects the kite to the KCU and takes up forces through multiple reinforced points. A bridle

line system is typically made of polyethylene with a high molecular ultra-weight or poly-aramid (38).

The components associated with the system control are the KCU and sensors. The KCU, also called the steering mechanism, controls the flight path of the kite. The sensors are located on the KCU and are necessary for control algorithms and data processing by triggering the steering inputs and computer chips (38).

The structural components include the tethered rope and launching and landing system. The tether is incorporated into an AWE system, instead of a tower utilized in conventional wind turbines. The tether connects the kite to the ground station and its main function is to reinforce aerodynamic forces of the wing and transmit the resulting tensile forces. A common material chosen for the tethered rope is Dyneema, which is ultra-high molecular weight polyethylene. Dyneema has tensile forces that are roughly ten times higher than steel-based ropes of a similar weight. The launching and landing system is an essential component for the aircraft/kite, and has a variety of designs, depending on the company (38).

The mechanical aspects include a drum and generator. There are two different types of generators, known as either on-board or ground-based. Figure 1 shows a ground-based generator, which converts mechanical power from the tethered rope into electrical energy. Traction power allows the tether to reel out from a winch connected to the generator (38).

The electrical power components generally involve a battery, inverter, and transformer. These components are necessary in order to adjust the characteristics of generated electrical power before transmitting through an entire wind farm or to the electrical grid (38).

2.1.2. Lift-Mode vs. Drag-Mode

AWE systems include a kite-like structure connected by a tethered rope to a ground station. AWE system technology can be split into two main categories known as lift-mode and drag-mode. The lift-mode system, also referred to as a pumping-mode system, consists of a ground-based generator, incorporating either a soft or rigid-kite, and converts mechanical energy into electrical energy. The production of power is possible through reeling of the tether from a winch via wing lifting forces and retraction during a specific time of flight (20). The drag-mode system involves a generator on-board the aircraft and incorporates a rigid-kite with attached turbines that transmit electric power to the ground station through a conductive tether. Electricity is continuously generated during a crosswind flight path in drag-mode systems (24).

There are many different designs of AWE systems, but for the purpose of this thesis only the companies with the highest levels of technological readiness will be discussed. Three specific AWE companies and their technology are represented in this work. Figure 2 represents the kite designs of (a) SkySails Power, (b) Makani Air, and (c) Ampyx Power. SkySails Power utilizes the lift-mode system and consists of a soft-kite with a ground-based generator. Makani Air incorporates the drag-mode system with a rigid-kite and onboard-generator, with mounted turbines. Ampyx Power utilizes the lift-mode system, with a rigid-kite and ground-based generator.

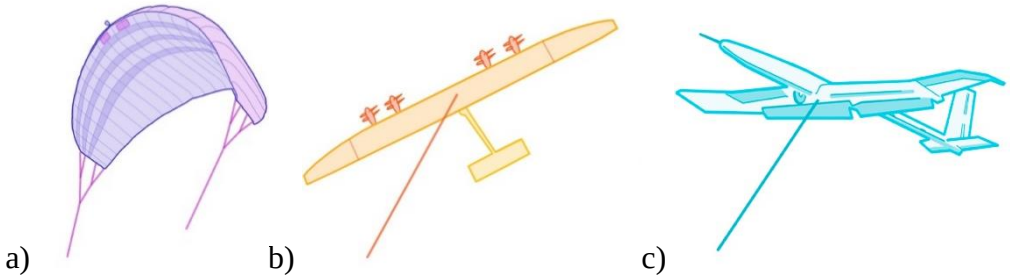

Figure 2. The most promising AWE design concepts. (a) Soft-kite design with lift-mode technology; (b) Rigid-aircraft design with drag-mode technology; (c) Rigid-aircraft design with lift-mode technology (9).

The flight trajectories and energy generation approaches differ between lift-mode and drag-mode systems. There are two phases of energy generation with lift-mode systems, involving the generation phase and recovery phase, which is represented in Figure 3. During the generation phase, the tethered rope unwinds while the aircraft performs its figure-eight crosswind flight to its final airborne position. A high tensioned force is exerted on the tethered rope by the kite. The recovery phase involves a specific flight path which uses fewer lifting forces to minimize consumed energy as the kite/aircraft returns to its resting position (20).

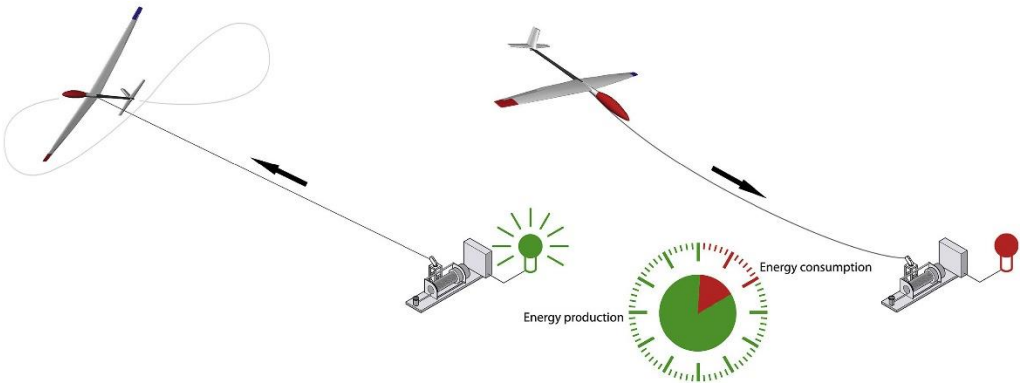

Figure 3. Basic two-phase energy production of a lift-mode AWE systems, consisting of the (left) generation phase and (right) recovery phase (20).

The drag-mode technology consists of an onboard generator and produces electricity differently, compared to lift-mode technology. Electricity is generated via aircraft mounted

turbines and its circular crosswind trajectory shown in Figure 4. Regardless of whether the AWE technology is a lift-mode or drag-mode system, the soft/rigid-kite is required to follow a cyclic patterned flight path to maximize production of net power for each complete cycle (24).

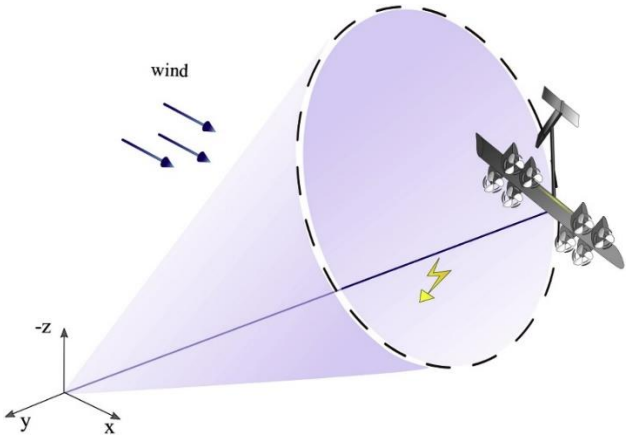

Figure 4. Energy production of a drag-mode system with a circular flight path (24).

2.2. Atmospheric Research for Airborne Wind Energy

Airborne wind energy systems convert wind energy into electricity through the utilization of air flow, particularly kinetic energy. A comprehensive understanding of wind power and its properties and how they interact with AWE systems is necessary when evaluating this new wind technology for energy generation on a global scale, and for determining ideal deployment locations. Specifically, determining estimations of wind resources at high altitude levels within the atmosphere is necessary when evaluating the economic potential of AWE.

2.2.1. Wind Power

Wind is generally represented as a vector due to its magnitude, involving wind speed and direction variables. In the case of an AWE resource analysis such as this one, the direction is insignificant since AWE systems can point themselves in the direction of the wind. Comparatively, wind speed is extremely significant when evaluating wind resources for AWE

technology because kinetic energy is a squared function of the wind speed. Thus, as the wind speed doubles, the kinetic energy increases by a factor of four, leading to a proportional change in the generated electricity output.

The hub height of conventional wind turbines is approximately 100 m above surface in the boundary layer, only accessing modest wind resources. This is due to friction and turbulence of the surface negatively impacting wind speed within this layer. The boundary layer extends up to 1000-1500 m in altitude, with more prevailing wind resources at increased height beyond this point. The empirical power law or the theoretical log law are commonly used to calculate wind speed in the boundary layer. When investigating wind speed above 500 m in height, the log law becomes inaccurate. Also, even though the empirical power method is widely used when evaluating wind speed, its accuracy is consistently doubted (3). The log law is defined as:

$$v_w(h) = v_w(h_{ref}) \frac{\log(\frac{h}{z_o})}{\log(\frac{h_{ref}}{z_o})} \quad (1)$$

h	*Height above ground*	[m]
h_{ref}	*Reference height*	[m]
z_o	*Roughness length*	[m]

Alternatively, wind resources above the boundary layer are dictated by geostrophic winds, due to approximate balance between the Coriolis force and pressure gradient force. Calculating the amount of power obtained from air passing through the blades at a specific cross section A, of a conventional wind turbine is determined by the wind speed (v) and density (ρ) functions (5). The power P (J s^{-1} or W) of available wind is stated as:

$$P = \frac{1}{2}\rho A v_w^3 \quad (2)$$

While conventional wind turbines are limited to a certain cross section, AWE systems span across a much larger volume. The wind power density (p_w) function is incorporated into the formula to determine the unit area when investigating wind resource potential for AWE technology and is defined as:

$$\delta = \frac{P}{A} = \frac{1}{2}\rho v_w^3 \quad (3)$$

The most essential wind property for analyzing wind resources for both conventional and AWE systems is wind power density (δ). It accounts for both wind speed and air density and these directly influence wind power production. Due to the existing cubic relationship between wind speed and wind power, the fluctuation of wind power is far greater than wind speed. Inaccurate forecasting or minuscule changes in wind speed will impact the extraction of wind power substantially (3).

2.2.2. Upper Atmospheric Winds

The dominating forces at high altitudes influencing wind are known as PGF (pressure gradient force) and Coriolis. The flow known as "geostrophic" is the result of these two forces balancing each other out at a given height in the atmosphere (>1000-1500 m) as the retarding effect of friction dissipates with height. The geostrophic wind vector (v_G) is expressed below as:

$$v_G = \frac{1}{f\rho} k \; x \; \nabla_h p \quad (4)$$

This simplified assumption of geostrophic flow works well when evaluating upper atmospheric levels, which surpass the boundary layer. The different atmospheric regions that AWE systems are exposed to daily in the boundary layer are illustrated in Figure 5. Conventional wind turbines mainly operate in the surface layer between 100-200 m, while AWE systems

operate in the Ekman layer, where flow is adjusted from the surface layer to geostrophic wind (5).

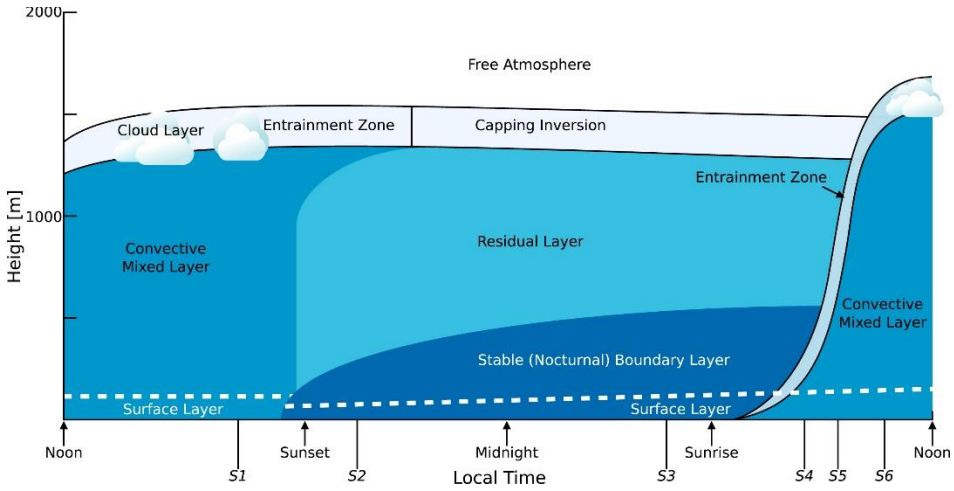

Figure 5. The three different regions of the boundary layer including the turbulent mixed layer, the less turbulent residual layer, and the expanding nocturnal boundary layer (5).

2.3. Competing Airborne Wind Energy Technology

Three companies with AWE technology based off the designs in Figure 2 include SkySails Power, Makani Air, and Ampyx Power. These companies are at the forefront of the AWE industry, concerning onshore and offshore design concepts and have all successfully generated electricity from onshore prototypes. They are each in different stages of testing their prototypes in offshore environments.

2.3.1. SkySails Power

Currently, SkySails is the only AWE company to reach the developing industrial application stage. The flex power mobile unit technology, which is a 200-500 kW system, is now available for small-scale applications. This technology is potentially useful for off-the-grid

locations, such as islands, private wind farms, and remote locations and industries in need of an alternative source of energy at a cheaper price.

The company's next step involves creating their onshore units, with 1-7 MW energy production. Their ideal applications include onshore wind farms and hybridizations of existing energy infrastructure such as island grids and solar farms. SkySails will also work towards reaching commercialization with their technology in an offshore environment. The offshore farms aim to range between 1-7 MW and consist of both stationary and floating design units, depending on depth of the offshore wind farm site (35). The company's onshore AWE system is shown in Figure 6.

Figure 6. Onshore SkySails technology with ground-based generator and soft-kite (35).

SkySails technology incorporates a soft-kite and ground-based generator. The system has two energy production phases displayed in Figure 7. During energy production, the kite pulls on the tethered rope connected to a winch system, which is connected to the generator. The recovery phase occurs once the rope achieves its maximum length and the kite is automatically adjusted to a position with very low tractive force. The rope is then rewound by the generator until the length is short enough to begin the production process again. The recovery phase uses only a

fraction of the energy generated from the energy production phase and the remaining energy is supplied to the power grid. When the system is not in use, the winch retracts the tether and returns the kite to the launch and recovery platform, which is lowered into a storage container (35).

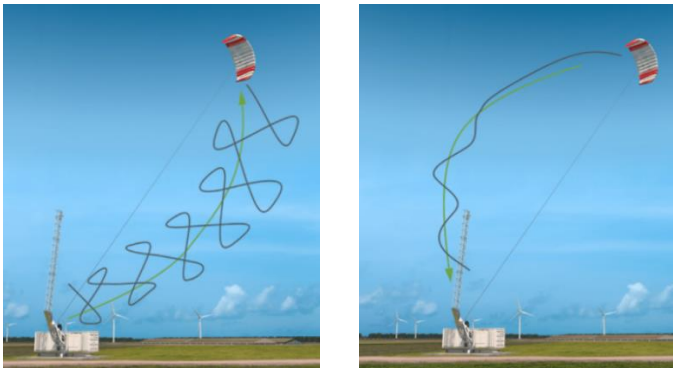

Figure 7. SkySails energy production process, consisting of the (left) energy generation phase with figure eight flight path, and (right) recovery phase (35).

The offshore design of their system claims to have about 25% less production costs, with a fast and low-cost installation process. The company has not created an offshore prototype, but plans to construct an AWE system with a compact ground station and foundation that has 90% less weight than a conventional floating offshore wind turbine. Their floating platforms are modeled after the spar-buoy design and will be further discussed in the following section. The company is aiming for water depths up to 700 m and will incorporate a storage container, making their design ideal in hurricane prone locations, such as the Gulf of Mexico (35).

Figure 8. Floating offshore SkySails technology design with Hywind floating platform concept (35).

2.3.2. Makani Air

Makani Air's most recent prototype, originally designed in 2014, is the M600 and has a wingspan of 26 m, and rated power of 600 kW. The company's AWE technology consists of a carbon fiber, rigid-wing with a superior-strength tether. It also incorporates an onboard generator, categorized as a drag-mode system, with eight energy-generating rotors (23). The company's prototype is shown in Figure 9.

Figure 9. Makani Air's onshore M600 prototype, with a 26 m wingspan, and 600 kW rated power (23).

The aircraft generates energy through its circular crosswind flight-path as the wind spins the system's onboard rotors. The tether component sends medium voltage power to the onboard

motor/generator incorporated into each rotor to launch the rigid-kite out of its stationary position. Once the kite is airborne and begins its crosswind flight path, the tethered rope allows the transfer of onboard-generated power to the electrical grid to take place. The flight path is possible using onboard computers, with incorporated flight controller software. Specifically, collected data from the onboard GPS and other sensors assist the software (23). The four energy production phases are represented in Figure 10.

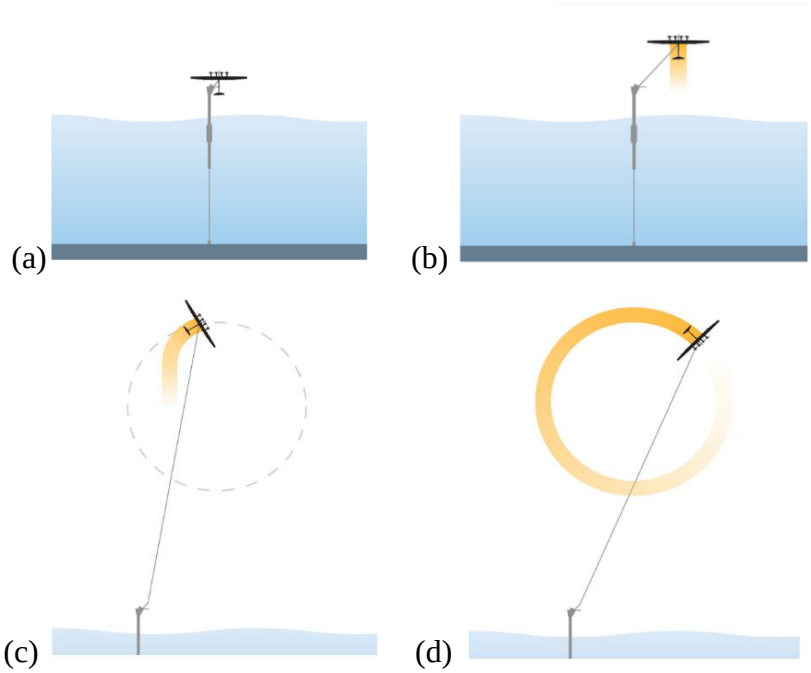

Figure 10. Visual representation of Makani Air's circular flight path and rigid-kite design with an onboard generator (23).

Makani Air is the only AWE company that has created an offshore prototype and successfully tested its capabilities. The first ever offshore demonstration flight of AWE technology took place in August of 2019, off the coast of Karmøy, Norway. The company's M600 prototype, with a 25 m wingspan, and 600 kW rated power was tested. The floating platform utilized in their offshore design also incorporates a spar-buoy design, similar to

SkySails. The company's recent partnership with Royal Dutch Shell allowed for AWE to finally take flight offshore (23). This was an important milestone in the commercialization of AWE in an offshore environment.

Figure 11. First ever tested offshore floating AWE system prototype in August 2019, developed by Makani Air in partner with Royal Dutch Shell, and modeled after the Hywind floating platform concept (23).

2.3.3. Ampyx Power

Ampyx Power's technology has a rigid-wing design and a ground-based generator. This AWE technology is categorized as a pumping-kite system and generates electricity through its figure-eight flight path. The company's most advanced prototype is the Model AP3, with a 12 m wingspan and twin fuselage system. The rigid-wing consists of a triple element design, with automated flaps and fixed slats, allowing maximum aerodynamic lifting to occur. The tether component is made from Dyneema DM20 material and has an overall length of 750 m. A diameter of 8 mm accounts for extended periods of friction-related wear. The ground-based generator and tethered drum produce power throughout the reel-out phase and force the drum to pull the tether to initiate the reel-in phase (1).

The energy production process for Ampyx Power's technology is like SkySails, other than the difference in kite design. Instead of a soft-kite, Ampyx incorporates a rigid-aircraft.

High tension pulls the tether from the winch and the wind assists the aircraft to a high-altitude position. The ground-based generator then converts the motion from the tether into electricity (1). A schematic of the figure-eight flight path, with a rigid-aircraft is represented in Figure 12.

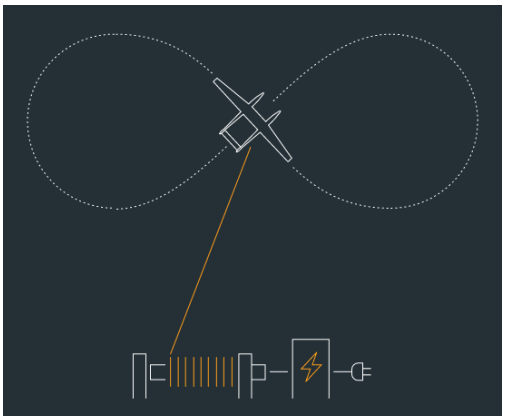

Figure 12. Illustration of figure-eight flight path, with a rigid-kite design and ground-based generator (1).

Ampyx Power has designed an offshore AWE system, but an actual prototype has not been created. The company aims to reach commercialization for both onshore and offshore AWE technology. Ampyx Power's first commercial product is their AP4 aircraft design, with a 150 m^2 wingspan (1). The floating platform chosen for their offshore system involves a semi-submersible platform, which is discussed in the following section.

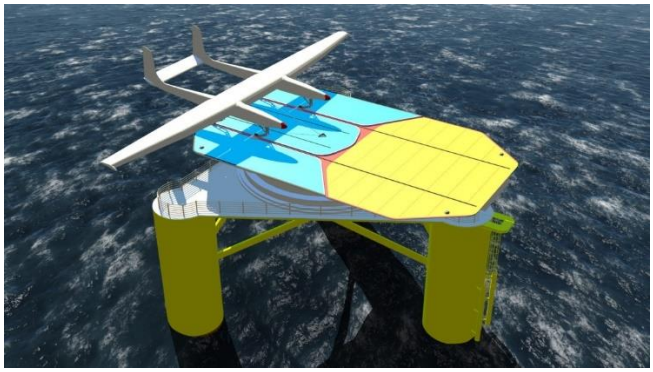

Figure 13. Ampyx Power floating offshore AWES design concept modeled after the WindFloat floating platform technology (1).

2.4. Floating Offshore Wind Platforms

Currently, the only research relating to floating and bottom-fixed offshore wind platforms involves those designed for conventional wind turbines. Until recently, only bottom-fixed offshore wind farms existed, while floating offshore wind farms were not a reality. This changed when the first floating wind farm, Hywind Scotland developed by Equinor, was commissioned in October of 2017, off the coast of Scotland. There are various floating offshore platform designs in existence, but they all fall into three general categories. The main categories consist of spars, tension leg platforms (TLP), and semisubmersible/hybrid platforms (29).

2.4.1. Floating Wind Platform Components

There are multiple types of floating platform concepts for a single-turbine and five have been analyzed in this work. Floating wind platforms consist of several components including the substructure, mooring system, and grid connection system. The wind substructures can be further classified by the type of mooring system associated with its overall design. The most common types of mooring systems used for floating oil and gas platforms and ship anchoring include catenary moorings, taut-leg moorings, and vertical tension legs (25)

The offshore substructure component is mainly constructed of welded and treated steel and represents a large percentage of total production costs analyzed in the following chapters. The three general categories previously mentioned include spars, taut-leg platforms (TLP), and semi-submersible substructures and are represented in Figure 14. The spar buoy design consists of a cylindrical ballast-stabilized substructure and has a lower center of gravity than center of buoyancy in the water column. The TLP design is stabilized through its mooring line tension and is partially classified as a semi-submerged system. The semi-submersible design is buoyant

stabilized and floats on the surface due to its semi-submerged substructure. This concept achieves stability through its weighted water columns (27).

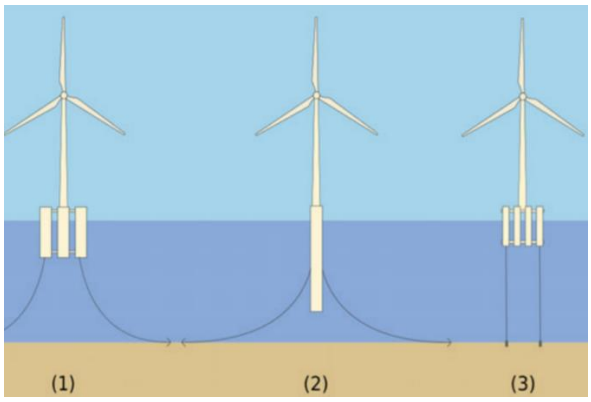

Figure 14. Three general floating substructure categories including. (1) Semi-submersible, (2) Spar-Buoy, and (3) Tension-Leg Platform (25).

There are three different types of mooring systems with the main two being catenary and taut-leg, while the vertical tension leg is a subset of the taut-leg system. Mooring systems consist of two main components, which include the seabed anchors and mooring lines. The mooring lines are either made from chain, cable, or pipe and connect the floating substructure to the anchors embedded in the seafloor. The catenary and taut-leg mooring systems are represented in Figure 15. An advantage of the catenary system is its ability for deployment in shallower water and lower anchor costs. A main issue with the catenary system is its insufficient vertical tension of the anchor line, leading to the higher probability of platform overturn. Taut-leg mooring systems are ideal for greater water depths since they have a smaller trajectory, requiring less mooring line length. The downside of this system is the high vertical anchor forces requiring costlier anchors with greater design complexity (37).

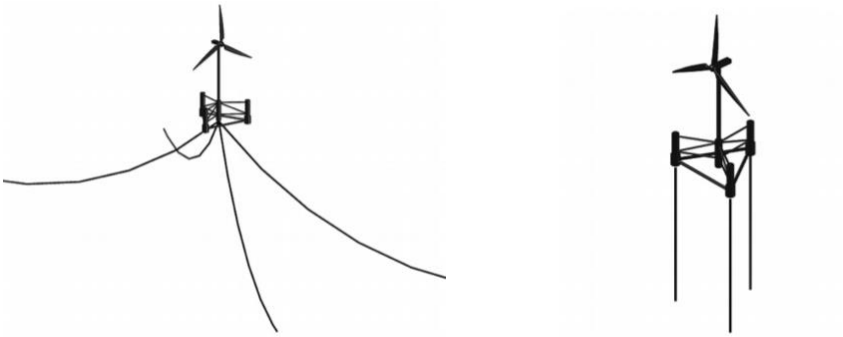

(a) Catenary Mooring System (b) Taut-Leg Mooring System

Figure 15. The two main types of mooring systems (39).

The soil condition of the seabed is an important factor when determining the appropriate anchor type at a potential wind farm site. Soil site conditions such as the weight and shear strength of the soil are necessary factors when installing anchoring systems. These factors vary greatly among sites, leading to most anchors being constructed for specific soil conditions. The different types of anchors consist of dead weight, drag embedment, pile, suction, and vertical load anchors, and are represented in Figure 16 (25).

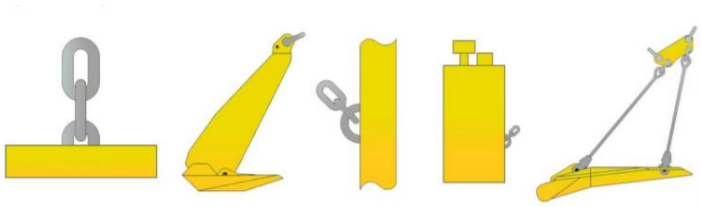

Figure 16. Various anchor types utilized for floating offshore platforms, starting on the far left with the dead weight anchor, drag embedment anchor, pile anchor, suction anchor, and vertical load anchor (6).

The grid connection system for an offshore wind farm consists of three main components including the inter-array cable, export cable, and substation. The inter-array cable connects the wind turbines to the offshore substation. Inter-array cables are short compared to the export cables. The inter-array cable is typically 1 km in length between each turbine in a conventional offshore wind farm. The export cable exists between the offshore substation and onshore

transmission system. This cable incorporates a conductor, usually consisting of aluminum or copper, an insulator, and a chemical and mechanical buffer. The cable can be either an AC export cable with three-part conductors, or a DC export cable with two single-core conductors. An offshore substation is necessary when a wind farm is situation more than 15 km from shore. It increases the voltage of the electricity produced from the offshore wind farm before it reaches the onshore substation (17). A general schematic representing the different HVAC and HVDC transmission systems for an offshore wind farm is represented in Figure 17.

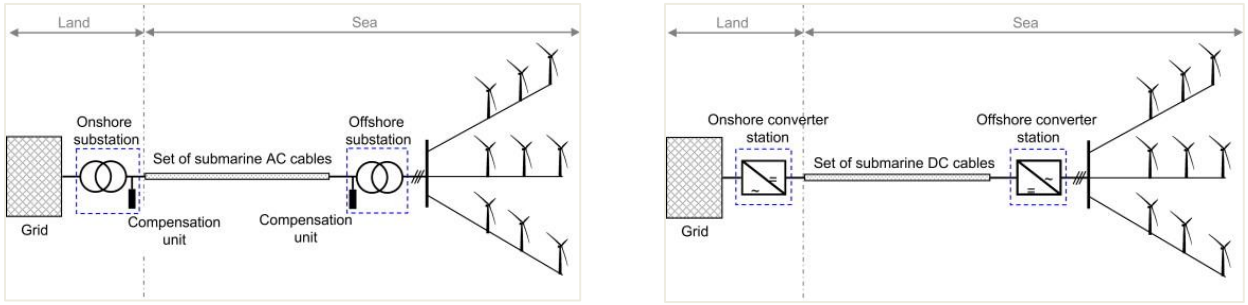

Figure 17. Schematics of a (left) HVAC transmission system and a (right) HVDC transmission system in an offshore environment, including the inter-cable, export cable, offshore and onshore substations, and electric grid (17).

2.5. Competing Floating Wind Platform Technology

For this thesis, five specific design concepts will be discussed to determine which has the lowest capital expenditures (CAPEX) and operational expenditures (OPEX). This will help determine which concept has the largest profitability alongside the AWE technology, by conducting an NPV cost model. The five design concepts include TLB-B, TLB-X3, Hywind, WindFloat, and SWAY and are represented in Table 1.

Table 1. Overview of competing wind turbine concepts (6).

	TLB-B and TLB-X3	***Hywind***	***WindFloat***	***SWAY***
Developer	UMB/IFE	Equinor (formerly Statoil)	Principle Power Inc.	Inocean (formerly SWAY AS)
Foundation Type	Tension-Leg-Buoy (TLB)	Spar-Buoy	Semi-Submersible	Tension-Leg-Spar (TLS)
Mooring	Taut leg system (6 lines)	Catenary system (3 lines)	Catenary system (4 lines)	Vertical system (1 line)
Water Depth	> 75 m	> 100 m	> 40 m	60 – 300 m
Substructure Weight	445/521 tons	1,700 tons	2,500 tons	1,100 tons (including tower)
Strength	Steel mass + draft + mooring footprint	Stability	Installation + draft + stability	Steel mass + mooring footprint
Challenges	Installation + mooring	Steel mass	Steel mass	Installation
Stage of Development	1:40 scale test in 2013	Commercial	Commercial	1:5 scale prototype in 2012

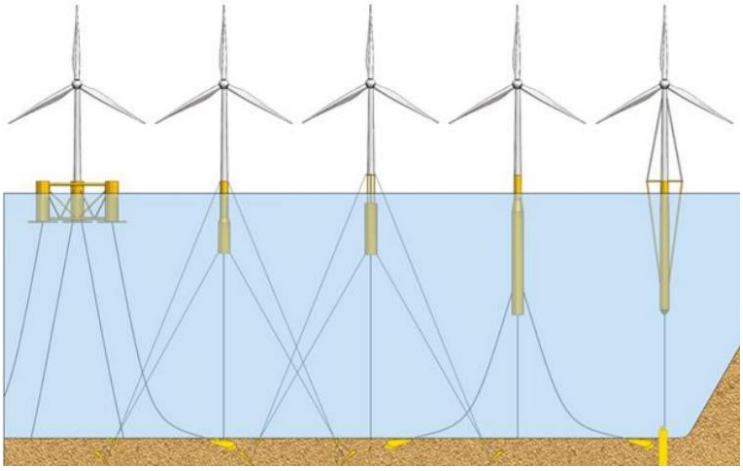

Figure 18. Visual representation of the five substructure design concepts. From left to right: WindFloat, TLB-B, TLB-X3, Hywind, and SWAY (6).

2.5.1. TLB-B and TLB-X3

The TLB-B and TLB-X3 design concepts are tension-leg buoy platforms and have been designed and investigated by the Norwegian University of Life Sciences and the Norwegian Institute for Energy Technology. Currently, these concepts have not surpassed their prototype testing stages that took place in 2013. Floating structures such as TLBs have many similarities to bottom-fixed structures due to their stiffness-controlled mooring systems. The TLB-B and TLB-X3 platforms have two sets of taut and inclined mooring lines connected at two different heights. The tension-leg buoy concept is expected to have significantly less steel mass and restricted dynamic response when compared with other platform concepts and are ideal for deployment at water depths of 75 m or greater. One drawback to this design would be the higher mooring costs compared to other concepts. The incorporation of the taut mooring lines leads to the anticipated higher mooring costs because of substantial anchoring loads, regarding wind and wave variations (27).

Figure 19. Conceptual design of the tension-leg-buoy (TLB) floating offshore wind platform (28).

There is a slight difference between the TLB-B and TLB-X3 designs that distinguishes them from one another. The shape of the floater, directly below the turbine tower boundary at 10 m above the water line, varies among each design. The TLB-B consists of a single conical shape, while the TLB-X3 shifts to three smaller pipes. Both TLB concepts were tested at a 1:40 scale in January of 2013 in Brest, France with the assistance of the MARINET (Marine Renewables Infrastructure Network for Emerging Energy Technologies) program. The results of the tests seemed promising regarding the overall performance of the floating platform concept. Extreme weather simulations were conducted on the smaller scale prototypes and produced positive indications of overall substructure stability. There has been little research conducted on these platforms since the original prototype testing in 2013 (28). Alternatively, other design concepts analyzed in this research, known as Hywind and WindFloat, have surpassed the tension-leg-buoy (TLB) design concepts by reaching commercialization.

2.5.2. Hywind

The Hywind floating platform was originally developed by Statoil (now Equinor) and is the company credited for creating the world's first floating wind farm. Hywind technology involves a single floating cylindrical spar-buoy with either a cable or chain-based mooring system. The entire structure floats upright due to its ballasted platform. Currently, Equinor is the leading developer in the world for floating offshore windfarms, since reaching commercialization in 2017. The company first began testing their technology with the deployment of a 2.3 MW turbine prototype, with an 85 m diameter, off the coast of Karmoy, Norway in 2009. The Hywind Demo was tested throughout a 6-year period, and provided

valuable data leading the company to proceed to the next phase of development in 2015, later resulting in the commercialization of their technology (18).

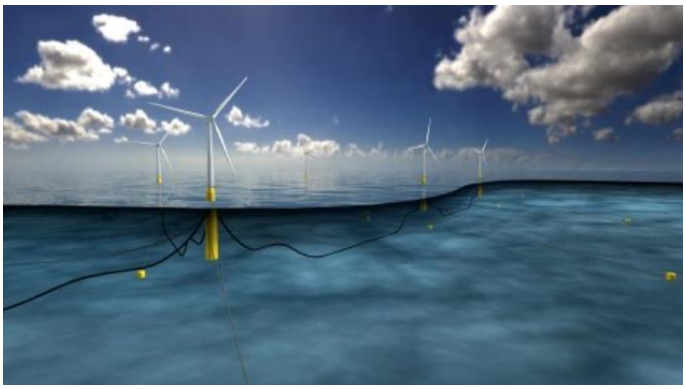

Figure 20. Visual representation of a Hywind offshore wind farm, highlighting it's ballasted catenary layout, with three incorporated mooring cables (18).

In October of 2017, Hywind Scotland became the world's first floating wind farm and consists of five 6 MW wind turbines and is shown in Figure 21. Hywind Scotland is a 30 MW system and is located 29 km off the coast of Peterhead, Scotland in Buchan Deep. Each floating turbine has a ballasted catenary system, three mooring cables, and 60 ton hanging weights. The weights provide additional tension at the midpoint of each anchor cable. The operation of each wind turbine is monitored through onboard control software to maximize production and dampen tower motion by altering the pitch of the blades when necessary. Also, a transmission system with underwater cables and a 33 kV voltage, successfully transfers produced electricity to shore and powers a total of 22,000 residences (18).

Figure 21. Hywind Scotland was the world's first floating wind farm, with five 6 MW turbines and is located 29 km offshore from Peterhead, Scotland (18).

Table 2. Parameter comparison between Hywind's prototype and their commercialized wind turbine technology (18).

Dimensions	***Hywind Demo 2.3 MW Karmoy, Norway***	***Hywind Scotland 6.0 MW Buchan Deep, United Kingdom***
Mass	5,300 tons	11,200 tons
Draught	100 m	78 m
Hub height	65 m	98 m
Water depth	220 m	105 m
Substructure diameter	8.3 m	14.4 m
Rotor diameter	85 m	154 m
Anchor	Drag embedded anchor	Suction anchor
Mooring	Wire/chain	Chain

Equinor Energy is currently in the process of developing their second floating offshore wind project in the Norwegian North Sea. The Hywind Tampen project will be the world's first ever renewable energy project responsible for powering offshore oil and gas platforms. The company operates two existing oil and gas platforms, known as Gullfaks and Snorre, in the Tampen area. Hywind Tampen will provide electricity to these offshore sites and will have a total capacity of 88 MW, consisting of eleven individual 8 MW turbines (18).

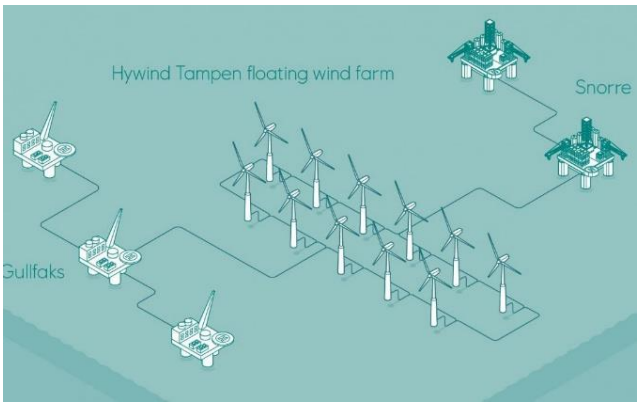

Figure 22. Schematic of the future Hywind Tampen floating wind farm designed to provide electricity to offshore oil and gas platforms (18).

2.5.3. WindFloat

The WindFloat design concept was developed by Marine Innovation and Technology and later commercialized by Principle Power. The WindFloat concept consists of a three-legged floating, semi-submersible platform, capable of supporting a 3-10 MW turbine in 40 m or greater water depths. The first prototype, known as WindFloat 1, was installed in offshore Portugal in December of 2011, and operated for 5 years (40).

Principle Power reached the commercialization stage with their semi-submersible technology in January of 2020. The wind farm consists of three 8.4 MW turbines, making them the largest turbines in the world on floating platforms. One of the 8.4 MW turbines during its installation process is represented in Figure 23. The WindFloat Atlantic wind farm has a total installed capacity of 25 MW and is located 20 km offshore from Viana do Castelo, Portugal (40).

Figure 23. One of the three 8.4 MW semi-submersible turbines during the installation process of the WindFloat Atlantic project, commissioned in January of 2020 (40).

2.5.4. SWAY

SWAY is a patented spar-type floating design concept and ideal for 60-300 m water depth locations. This technology was developed by the Norwegian company, Inocean (formerly SWAY AS), and has not evolved past its prototype testing stage, conducted in 2012. The concept has a tension-torsion leg, anchored to the seabed and a passive subsea yaw swivel. This platform is categorized as a hybrid system, combining tension leg platform (TLP) technology with a self-stabilizing ballast. SWAY is designed to handle a turbine capacity between 2.5 – 5 MW. A notable characteristic of this design concept is the low-material consumption, with 50% less cost estimates, compared to most offshore floating platforms (36).

Figure 24. Illustration demonstrating the SWAY floating turbine design concept (36).

Chapter 3. Methodology

This work is based on the master thesis of Catho Bjerkseter and Anders Agotnes at the University of Life Sciences in Norway from 2013, and the updated version of their results conducted by Dr. Anders Myhr, published in 2014 (26). The data incorporated into this techno-economic analysis from these sources provides critical life cycle costs in relation to five different floating offshore wind platform concepts, originally designed for a 5 MW conventional turbine. The estimated life-cycle costs originating from these published sources have been downscaled to accommodate a lighter 2 MW AWE system. Additionally, this work is based on the research of Dr. Pietro Faggiani and Dr. Roland Schemhl of Delft University of Technology in the Netherlands and utilizes the estimated production cost data of a generic onshore AWE system (14). The power curve and yield estimation data of a theoretical airborne wind turbine, from the work of Dr. Maximilian Ranneberg at EnerKite, is applied to the economic feasibility cost model (30). The goal of this work is to develop data from published literature to generate NPV cost models and sensitivity studies for project value of a 500 MW floating offshore AWE farm, with 250 individual 2 MW AWE systems and five different floating platform concepts in the Gulf of Mexico.

A life cycle cost assessment (LCCA) was developed from these sources and used to estimate capital expenditures (CAPEX) and operation expenditures (OPEX) of a hypothetical utility-scale AWE farm designed off the coast of Venice, Louisiana. The capacity factor of AWE was also used from the power curve and yield estimation data literature and incorporated into all NPV cash flow analyses. Once the NPV cost models were completed for the five floating wind

farm concepts, multiple sensitivity input variables were applied to establish NPVs for all floating wind farm concepts to determine future investment potential.

The goal of this section is to establish the various methodologies used in this thesis. This section includes the methods used in the *Techno-Economic Analysis*, subdivided into the *Goal of Work, General Conditions, Life Cycle Cost Assessment, Wind Resource Analysis, Economic Feasibility Cost Model, and Sensitivity Study.*

RQ 1: Is the high-altitude wind speed in the Gulf of Mexico adequate to support airborne wind energy (AWE) systems?

RQ 2: Are utility-scaled offshore floating airborne wind energy (AWE) system projects worth investing in?

To address these questions and achieve the established research objectives, Figure 25 represents the methodology processes involved in this techno-economic analysis discussed in the following sections.

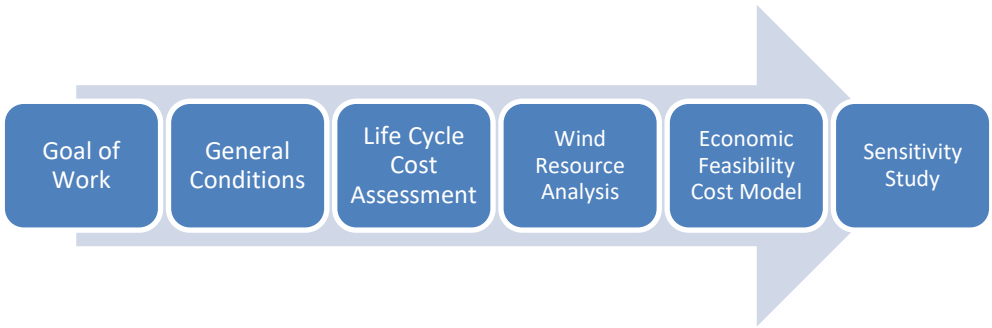

Figure 25. Methodology process for a techno-economic analysis of a utility-scale, floating offshore airborne wind farm.

3.1. Goal of Work

There are several goals pursued in this techno-economic analysis of floating (AWE) systems, which consists of multiple sub-analyses. The first analysis involves the LCCA conducted on each floating platform, downscaled to accommodate a lighter AWE system. Secondly, a wind resource analysis is completed for high-altitude wind speed at a hypothetical wind farm site, 15 km offshore from Venice, Louisiana. The importance of the wind resource analysis is to observe overall wind speed potential between 100-1500 m in altitude. Thirdly, an economic feasibility cost model is conducted for the hypothetical wind farm with a total capacity of 500 MW, testing the five design concepts. Specifically, a cash flow analysis took place using the NPV method, which incorporates data collected from the LCCA, to determine the CAPEX and OPEX. The wind speed potential is analyzed from the high-altitude wind resource analysis performed at the hypothetical wind farm location, but the capacity factor and other parameters necessary for the NPV cost model were attained from published literature. Lastly, a sensitivity study is completed to further determine which floating wind farm concepts are worth the investment when key cost factors are adjusted.

3.2. General Conditions

The purpose of this section is to explain common conditions for each of the analyzed floating platform concepts. General conditions involved in all analyses for the five platforms are the wind farm parameters including, distance from shore, soil conditions, and water depth. Additionally, a general lift/pumping-mode AWE system is incorporated on each platform design. The general parameters, reference power curve, and reference yield and capacity factor associated with a lift/pumping system are each explained below.

3.2.1. Wind Farm Parameters

Hypothetical scenarios with floating offshore airborne wind farms were conducted consisting of 250 individual 2 MW AWE systems, incorporated with five different platforms design concepts, resulting in total wind farm capacities of 500 MW. The benchmark distance from port to the offshore farm was set to 15 km for all tested scenarios at a water depth of approximately 50 m, located inside state-water boundaries. For minimalism, a square-array layout of the wind farm is utilized. Temporal variability concerning wind direction and kite flow interaction was not considered. There are two inflow scenarios represented in Figure 26 where the systems are aligned according to wind direction and arranged in columns, while the systems in a perpendicular layout are grouped into rows (32).

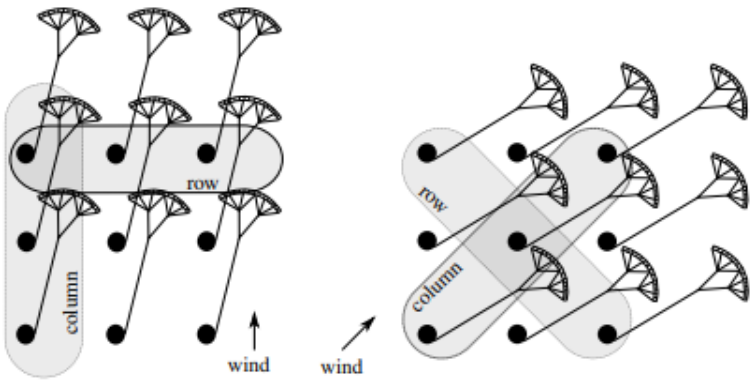

Figure 26. AWE systems arranged into columns with array design (left) and systems arranged into rows in diagonal to array design (right) (32).

Table 3. Site parameters for hypothetical airborne wind farm.

General Wind Farm Parameters	
Years of development	2030-2032
Commission year	2032
Project life span	30 years
Number of wind turbines	250 units
Size of wind farm	500 MW
Turbine type	Generic 2 MW
Water depth	50 m
Distance to nearest construction and operation's port	15 km
Site sediment conditions	Terrigenous Clay

An exact location for the offshore wind farm is set 15 km off the coast of Venice, Louisiana. The soil sediment characteristics for the entire Gulf of Mexico are shown below in Figure 27, with terrigenous clay existing offshore of eastern Louisiana, where the hypothetical wind farm is located (13).

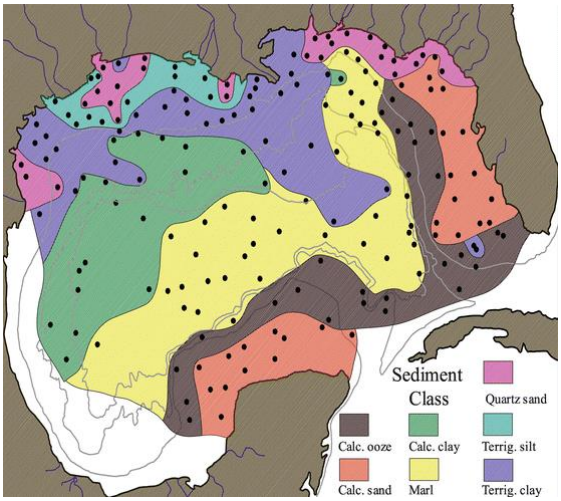

Figure 27. Sediment profile of the Gulf of Mexico, with terrigenous clay existing at the hypothetical airborne wind farm location (13).

3.2.2. Airborne Wind Energy System Parameters

All floating platform concepts incorporate a generic 2 MW AWE system, represented in Figure 28. A lift/pumping kite power system designed for utility-scale energy generation is utilized in this work from literature. The physical properties of a generic utility-scale AWE system were applied in the LCCA, concerning the total production costs. The design parameters of the generic system are detailed in Table 4.

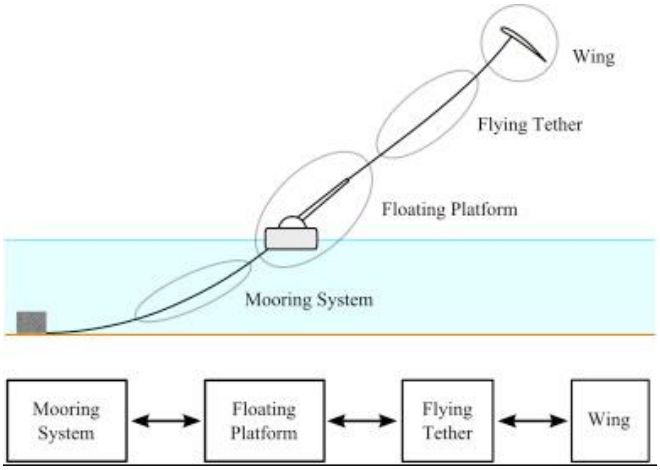

Figure 28. Basic design of floating offshore AWE system components (10).

Table 4. Generic AWE system parameters of a pumping kite system for utility-scale application (14).

Parameter name	***Symbol***	***Value***	***Unit***
Total wing surface area	A_k	100	m^2
Projected wing surface area	S_k	72	m^2
Kite mass	M_k	48	kg
Kite control unit mass	M_{kcu}	16	kg
Maximum wing loading		450	N/m^2
Tether diameter	d_t	12	mm
Aerodynamic life coefficient	C_L		
• Retraction phase		0.3	
• Transition and traction phases		0.8	
Aerodynamic drag coefficient	C_D		
• Retraction phase		0.1	
• Transition and traction phases		0.2	

3.2.3. Energy Production

An important aspect to understand about the electricity generation of AWE systems is that it will not always produce its rated power, due to various reasons including, poor weather conditions, mechanical issues, and electrical failures. Knowledge about the power curve, estimated yield, and capacity factor is vital concerning the energy production of AWE technology.

The power curve is the determining factor of performance for calculating the economic viability of an AWE system. The power curves of conventional wind turbines have been understood for decades, but the power curve estimation and optimization of drag-mode and lift/pumping-mode AWE still require extensive research. Currently, the power curve of a lift/pumping kite system has been tested and represented in literature. The reference capacity factor utilized from literature in this thesis is discussed below.

The reference capacity factor of AWE utilized from literature was compared to conventional wind in existence today. An EnerKíte 100 kW system is equated with two conventional wind turbines, which are the Fuhrländer FL100 turbine and the Siemens SWT-2.3 113. The comparison between the AWE system and the two conventional wind turbines is represented in Table 5. The rated wind speed is specified at hub-height for conventional wind turbines and defined at 200 m for AWE systems. The reference yield is determined for a five-year period by using a Rayleigh distribution, logarithmic wind profile with a 0.1 terrain roughness, and a 5.5 m/s wind speed at 30 m in altitude, based on the German Renewables Energies Act (EEG). A calculated yield of 95% is applied, due to the novelty of AWE systems, while 98% is utilized for a conventional wind turbine. The calculated reference yield is about

3,000 MWh with an annual yield of 600 MWh. Under the previously mentioned reference conditions, a capacity factor of 68% is obtained by dividing annual yield by nominal power (30).

Table 5. Comparison of an AWE EnerKíte 100 kW system with two conventional wind turbines (30).

	EnerKíte 100 kW System	Fuhrländer FL100	Siemens SWT-2.3 113
Rated Power (kW)	100	100	2,300
Rated Wind Speed (m/s)	7.5	13.0	11.5
Hub Height (m)	80-300	35	92.5-122.5
Capacity Factor (%)	68	24.3	41.5-44.3

3.3. Life Cycle Cost Assessment

The NPV cost models were carried out for each of the five platform concepts, investigating multiple scenarios with differing variables. The economic feasibility cost model was based on literature, involving the life cycle cost assessment (LCCA) approach. The LCCA is broken down into five different life cycle phases of a conventional floating offshore wind farm and was applied to a floating airborne wind farm. The five phases involved in an LCCA are represented in Figure 29. Only certain data and methods from published literature were utilized and necessary to conduct the NPV cost models for floating offshore airborne wind energy projects in the Gulf of Mexico.

Figure 29. Life Cycle Cost Assessment (LCCA) conducted on each floating platform design concept.

3.4. Wind Resource Analysis

The wind data was acquired from ECMWF and is ERA5-Reanalysis pressure level data. This dataset provides hourly estimates of many different atmospheric variables such as wind and geopotential data with a .25 x .25 resolution at 37 pressure levels. The available data ranges from 1979 to present (11). ERA5-Reanalysis data is the most reliable source to determine atmospheric winds to conduct this wind resource analysis.

In order to calculate wind speed at different altitude levels between 100-1500 meters (m), u-wind and v-wind components and geopotential data were downloaded for a 41-year time period (1979-2019) to generate the most accurate wind resource results. Once the data was downloaded using the Python scripting language platform, NCAR Command Language (NCL) was used to convert the barometric pressure levels to altitude levels. After the wind data was converted to altitude levels, data analysis took place using R-programming. Wind speed potential at different altitude levels was analyzed to produce graphs at a base case of 100 m, and at 300 m, 500 m, 1000 m, and 1500 m at the wind farm case study site in offshore Louisiana.

The two-parameter Weibull distribution method (abbreviated pdf) was utilized to accurately represent the mean wind speed at the tested site, since averaging the wind speeds underestimates power output. This is the best method to analyze measured wind speed data and the two-parameter formula is derived from Ref. (21):

$$F(v) = \frac{k}{c}\left(\frac{v}{c}\right)^{k-1}\exp\left(-\left(\frac{v}{c}\right)^{k}\right), k > 0, v > 0,\ c > 1 \quad (6)$$

Where:

c = Scale parameter (m/s)

k = Dimensional shape parameter

The power output and capacity factor of AWE systems are calculated in a different and more complex manner compared to conventional wind turbines. Due to time constraints involved in calculating the power output from the specific wind speed data evaluated in this thesis, a reference capacity factor of 68%, detailed in the previous section, was used for the economic feasibility cost model. The sourced capacity factor utilized the logarithmic formula, which is used when measured data is not available. Ideally, the capacity factor would be calculated from the measured wind data obtained for the tested site, but that was outside the scope of this research.

3.5. Economic Feasibility Cost Model

The extensive data collection process led to conducting various individual analyses to complete a techno-economic analysis of floating airborne wind energy systems in offshore Louisiana. After the necessary data collection took place, the techno-economic analysis began with the LCCA and high-altitude wind resource analysis. Once the life-cycle costs of a floating airborne wind farm were estimated and the wind resources were analyzed, the economic feasibility cost model was completed for all five design concepts and the NPV method applied is discussed below.

3.5.1. Net Present Value

To study the economic effects of floating AWE systems, the completion of the LCCA and high-altitude wind resource analysis were necessary to conduct an economic feasibility analysis for a hypothetical 500 MW offshore wind farm in the Gulf of Mexico. After the CAPEX and OPEX costs were estimated, a cash flow analysis was conducted to determine the net present value (NPV) for the differing floating wind farm concepts. There are many crucial parameters

incorporated into a cash flow analysis. The parameters include the total wind farm capacity, construction phase (years), total overnight capital cost (CAPEX), variable operations and maintenance (OPEX), capacity factor, electricity price, nominal growth rate of electricity sale price, discount rate, tax rate, and cost of debt. The CAPEX and OPEX estimates were all calculated from the LCCA, while the discount rate, tax rate, and cost of debt parameters were obtained from reliable capital cost data (12). The following formula is used to calculate the NPV and is derived from Ref. (33):

$$NPV = \sum_{t=1}^{n} \frac{R_t}{(1+i)^t} \quad (7)$$

Where:

$R_t =$ Net cash flow – outflows during one single time period t

$i =$ Discount rate or return that could be earned due to alternative investments

$t =$ Amount of timed periods

The NPV is the difference between the expected cash inflows and the expected cash outflows at present values throughout a time period. The significance of using NPV in this work is to analyze the profitability of a projected investment in offshore floating AWE systems on a commercial scale. When a positive NPV results, the projected earnings produced from the project exceed the anticipated costs of the project in present dollars. A resulting positive NPV assumes that a project will be profitable, while a negative NPV indicates the potential for net loss. This concept is the basis for the Net Present Value Rule, which indicates that only positive NPV projects should be considered for investment. A break-even analysis was conducted on the wind farm concepts that produced a negative NPV. This analysis tested different cost factors to

determine the ideal input values to reach an NPV of zero, where total revenue equals total expenses (33).

3.6. Sensitivity Study

The sensitivity study incorporates multiple input variables in terms of economic feasibility of a floating offshore airborne wind farm, further testing the profitability of five floating platform concepts. It displays how much the output variables are impacted due to changing the input variables. Only certain cost factors were analyzed in the sensitivity study, which are discount rate, CAPEX, OPEX, electricity price, and electricity production. Furthermore, the discount rate was increased up to 24%, both CAPEX and OPEX were increased up to 40%, cost of electricity was increased and decreased by $0.01, and capacity factor was increased by 10%, and decreased up to 20%.

Chapter 4. Life Cycle Cost Assessment

This section aims to evaluate the total life cycle costs for offshore airborne wind farms with five different floating platform concepts. All results from this LCCA were sourced from the previously mentioned literature. The LCCA consists of five different life cycle phases and are represented in Figure 30. Results from this LCCA for an individual 2 MW floating offshore AWE system, and a hypothetical 500 MW offshore floating airborne wind farm with 250 AWE systems, will be assessed and applied to the Net Present Value (NPV) cost model and sensitivity study carried out in Chapter 5.

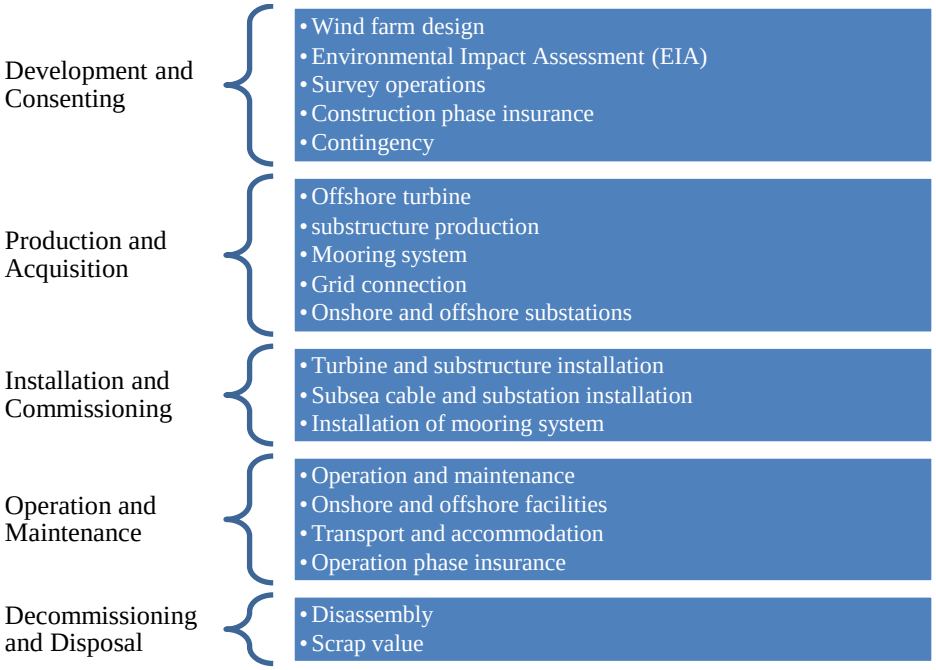

Figure 30. Breakdown of life cycle phases when evaluating a wind farm project (6).

4.1. Adjustments

The estimated costs in this LCCA were adjusted from Euros to U.S. dollars for a single time period (1 January 2019). The inflation rate is also an important aspect to consider when utilizing published data from previous years and two different options can be implemented. The estimated life cycle costs in this study were developed from two studies published in 2013 and 2018. Since exchange rates from each year vary between months, the order exchange rate adjustments and inflation rates applied can produce different results. Inflation can be applied to estimated project costs through the inflate-first or the exchange-first method. The inflate-first method inflates project costs from the construction year to the present in the original currency and then exchanges them to U.S. dollars. The exchange-first method exchanges the original currency to U.S. dollars and then applies the U.S. inflation index (19). The exchange-first method was implemented throughout this cost analysis. The exchange rate was first applied to the floating platform sourced data by adjusting cost estimates from 2013-Euros to 2013-U.S. Dollars.

$$\frac{\boldsymbol{USD_{2013}}}{\boldsymbol{Euro_{2013}}} = \mathbf{1.3192} \quad (8)$$

Then the exchange rate was utilized for the AWE system sourced data by adjusting cost estimates from 2018-Euros to 2018-U.S. Dollars.

$$\frac{\boldsymbol{USD_{2018}}}{\boldsymbol{Euro_{2018}}} = \mathbf{1.1792} \quad (9)$$

The *Producer Price Index (PPI)* was estimated to determine the inflation of each phase in the LCCA (8). The inflation for all cost estimates involving the floating platform components of the five design concepts were calculated using the PPI formula below.

$$\frac{PPI_{2019}}{PPI_{2013}} = \mathbf{1.0155} \quad (10)$$

The inflation rate for all cost estimates relating exclusively to the AWE system components were determined using the PPI formula below.

$$\frac{PPI_{2019}}{PPI_{2018}} = \mathbf{1.0005} \quad (11)$$

4.2. Development and Consenting

There are costs associated with wind farm projects before installation starts and these involve costs related to planning and development. This is a long-lasting phase and initiates with a political verdict to approve the desired wind farm in a specific area, which can begin up to five years before installation. Various procedures, studies, and paperwork are associated from the start for the potential project and are essential steps to determine its economic and technical feasibility. The costs associated with the development and consenting phase consists of the overall wind farm design, an Environmental Impact Assessment (EIA), conducting of surveys, construction phase insurance, and contingency (26).

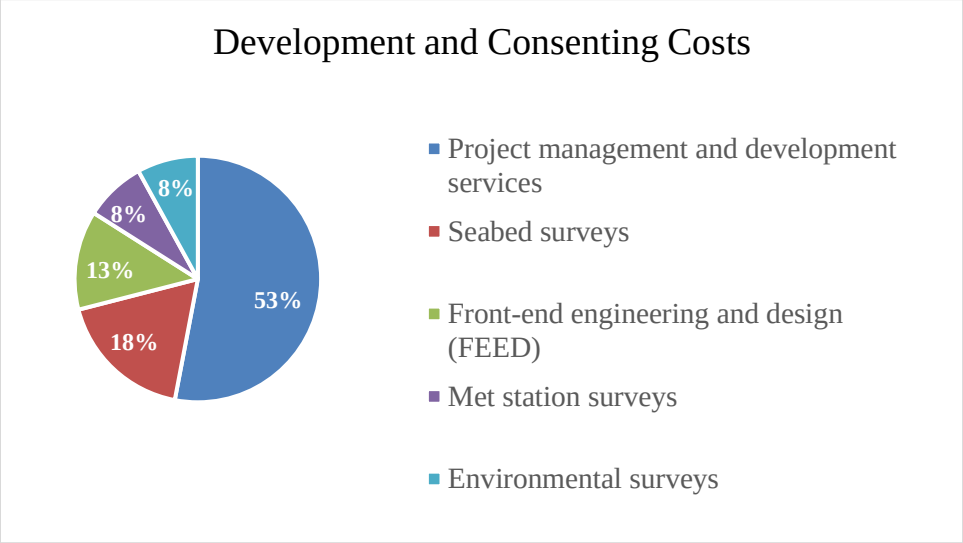

Figure 31. Different costs associated with the development and consenting phase (26).

Table 6. Cost breakdown of development and consenting costs for a hypothetical 500 MW offshore wind farm (26).

Development and Consenting Breakdown	***Costs ($)***
Project management and development services	*M$* 74.5
Seabed surveys	*M$* 25
Front-end engineering and design (FEED)	*M$* 17.9
Met station surveys	*M$* 11.5
Environmental surveys	*M$* 10.6
Total costs	***M$* 139.5**

4.3. Production and Acquisition

The production and acquisition phases include the manufacturing of each individual component making up a floating airborne wind farm. The production costs of all components associated with a single utility-scale AWE system were first estimated. The AWE system components include the electrical machines, drum, power electronics, transformer, tether handling and bearings, cover frame, launching and landing, kite, kite control unit, tether rope, electrical connections, and controls (14). The production costs of a floating airborne wind platform for the TLB-B, TLB-X3, Hywind, WindFloat, and SWAY design concepts were then estimated. The mooring systems at a 50 m depth for all five platforms and a grid connection 15 km offshore, were included in the production cost analysis. A substation is unnecessary for wind farms developed 15 km or less offshore and was not included in this LCCA. All estimated costs derived from the floating platform literature were downscaled from 5 MW floating conventional turbine platform concepts, to accommodate the lighter AWE system (26).

4.3.1. AWE System

All five floating platforms are assumed to be installed using a 2 MW AWE system based on a theoretical utility scale system. The cost values in Table 7 were adapted from airborne wind systems using kites with a surface area of 100 m^2 and a nominal power of 100 kW (14). The production costs of a 2 MW AWE system are relatively low, but the mature technology cost was calculated in the sensitivity study and used to determine overall investment potential for each wind farm concept.

Table 7. Production costs of a 2 MW AWE system (14).

Generic 2 MW Onshore AWES Components	***Costs ($)***
Electrical machines (generator)	$ 18k
Drum	$ 3.8k
Power electronics	$ 2.8k
Transformer	$ 5k
Tether handling and bearings	$ 10.8k
Cover frame	$ 360
Launching and landing	$ 5.8k
Kite	$ 26.4k
Kite control unit	$ 3.6k
Tether	$ 10.8k
Electrical connections	$ 27.6k
Controls	$ 3.6k
Total costs	**$ 118.6k**

4.3.2. Floating Substructure

The production cost estimates for the five concepts are provided in Table 8. The total production costs were modified from original estimates, which incorporated a conventional 5 MW conventional turbine. All material and manufacturing costs were downscaled by 3.5 to accommodate the lighter 2 MW AWE system. Platform concepts were decreased by this amount

based on an offshore floating platform simulation incorporating a 2 MW AWE system, known as the Sea-Air-Farm Project, completed by Ampyx Power in partnership with ECN (Energy Research Center Netherlands), Marin (Marine Research Institute Netherlands), and Mocean Offshore (2). The simulation involved a downscaled version of the Hywind platform with an Ampyx Power 2 MW AP-4 system. The downscaled Hywind platform in the simulation is a spar buoy with a three-column semisubmersible design, with a structural mass of 491 tons. The structural mass of a Hywind platform with a 5 MW conventional turbine is approximately 3.5 times more than the platform in the simulation, at 1700 tons. The same production cost estimate was applied to the other platform technologies. The material costs of each platform are based on the bulk price of steel and a complexity factor is applied to each manufacturing cost (6). Considering a mature industry with large-scale production, the total production costs are represented as the sum of material costs and manufacturing costs for each concept.

Table 8. Production costs for each floating platform concept.

Concept	***TLB-B***	***TLB-X3***	***Hywind***	***WindFloat***	***SWAY***
Material consumption (tons)	127	149	486	714	314
Material costs ($)	$ 127k	$ 149k	$ 486k	$ 714k	$ 314k
Manufacturing complexity factor (%)	110 %	130 %	120 %	200 %	150 %
Manufacturing costs ($)	$ 139.7k	$ 193.7k	$ 583.2k	$ 1428k	$ 471k
Total production costs ($)	**$ 266.7k**	**$ 342.7k**	**$ 1069.2k**	**$ 2142k**	**$ 785k**

Total production costs displayed in Table 8 suggests WindFloat has the costliest platform, due to its large steel consumption and complex design structure. The platform with drastically lower total production costs is the TLB-B, due to low steel consumption and simplistic design. However, production costs for other necessary offshore components, such as

the mooring system counteract the low costs of the TLB concepts discussed in the following section.

4.3.3. Mooring System

The purpose of a mooring system is to secure a floating structure in place at a specific site. The three categories of mooring systems represented in this thesis are catenary, vertical, and taut leg mooring systems. The seafloor soil and water depth at a benchmark offshore wind farm location are important factors concerning the production costs of a mooring system. The soil type at the wind farm site in offshore Louisiana consists of terrigenous clay and has a 50 m water depth. Advanced anchors are considered for each platform due to their deployment at utility-scale. Alternatively, dead weight anchors which are container shaped and filled with scrap metal, can be a cheaper option compared to advanced anchor systems. Dead weight anchors are one tenth the cost of advanced anchors, but they are not practical for commercial-sized projects where each anchor supports a vertical carrying capacity of 500-1000 tons (26). The sourced literature did not utilize dead weight anchors in their work due to using heavier conventional wind turbines on each floating platform concept. The anchors used in this work are advanced systems and they were downscaled by a tenth of the original costs, due to the practicality of using scrap steel for anchors supporting much lighter platforms and AWE systems. The baseline anchor costs are listed in Table 9 and show the type of anchor, total mass, complexity factor, and number of anchors associated with each concept. The total anchor costs for both TLB concepts and SWAY are high compared to Hywind and WindFloat concepts.

Table 9. Baseline anchor costs for each concept downscaled to accommodate a 2 MW system.

Concept	*Type*	*Mass (tons)*	*Complexity*	*Amount (n)*	*Total Cost ($)*
TLB-B	Stevmanta VLA	40	870 %	3	**$ 139.7k**
TLB-X3	Stevmanta VLA	36	870 %	3	**$ 125.7k**
Hywind	Stevshark Mk5	17	670 %	3	**$ 45.8k**
WindFloat	Stevshark Mk5	17	670 %	4	**$ 61.1k**
SWAY	Suction pile	140	1025 %	1	**$ 192.2k**

The mooring lines are used to connect the anchor to the floating platform, and different types can be used. The different mooring lines discussed in this work include chains, wired rope, synthetic fiber rope, and a combination of each type. The total line length and line costs provided in literature were estimated for mooring systems in 200 m water depth (26). The hypothetical wind farm is situated in 50 m water depth, with the total line lengths and line costs for each design concept being decreased by one fourth of the cost estimates found in literature. The total line costs in Table 10 show that the TLB-B and TLB-X3 concepts are considerably more expensive.

Table 10. Estimated line length and costs for hypothetical offshore windfarm at 50 m depth.

Concept	*Total Line Length (m)*	*Total Line Cost ($)*
TLB-B (upper fiber rope)	239	**$ 145.3k**
TLB-B (lower fiber rope)	203	**$ 147.6k**
TLB-X3 (upper fiber rope)	239	**$ 141k**
TLB-X3 (lower fiber rope)	203	**$ 200.9k**
Hywind (steel wire)	450	**$ 27.1k**
Hywind (chain)	38	**$ 12.6k**
WindFloat (steel wire)	660	**$ 39.8k**
WindFloat (chain)	50	**$ 16.7k**
SWAY (steel cylinder)	25	**$ 64.1k**

The platforms with the most expensive mooring systems, including all associated anchors and lines, are $432.6k for the TLB-B and $467.6k for TLB-X3. The SWAY concept has a mooring system cost of $258.3k, due to its high-priced suction pile anchors. The total mooring system costs for the Hywind and WindFloat platforms are reasonably priced at $85.5k and $117.6k. The concept with the cheapest mooring system is Hywind, which utilizes three Stevshark Mk5 anchors and steel wire and chain mooring lines.

4.3.4. Grid Connection System

The electrical components that are essential for an offshore wind farm include the inter-array cable, export cable, and substation, depending on distance from shore. The production costs per km and total costs for the hypothetical wind farm are presented in this section. A substation is not necessary for the purpose of this work and is not represented in total grid connection costs. The inter-array cable is subdivided into 20 rows, each connecting 10 AWE systems with a 300 mm^2 copper core conduction cable at 33 kV. There is a 1 km distance between each AWE system in the wind farm and the inter-array connecting lengths are approximately 1.4 km (6). The export cables are substantially larger and more costly than inter-array cables. In Ref. (26), the analysis focuses on a benchmark wind farm that is 200 km offshore and utilizes Direct Current (DC). The work of this thesis focuses on a wind farm much closer to shore, but Alternating Current (AC) is still not considered. The installation costs in Ref. (17) involves a sensitivity study closer to shore, leading to the usage of their grid connection estimates. A single 320 kV 1500 mm^2 High-Voltage DC system is chosen for the export cable (6). The inter-array cable and export cable costs per km of cable are $376.4k/km and $593.4k/km. The hypothetical wind farm is 15 km offshore, resulting in total production costs of

M$5.65 and *M*$8.9 for the inter-array cable and export cable. The total grid connection production costs are further represented in Table A-2 in Appendix A.

4.4. Installation and Commissioning

The total installation costs for floating airborne windfarms are discussed within this section. The most economically feasible option for each of the five concepts was chosen, which involves inshore turbine assembly in two components. Since this LCCA is based off a 5 MW conventional wind turbine, the cheapest installation strategy was chosen. Specifically, the 1D strategy was used and downscaled to accommodate a floating 2 MW AWE system (26). The installation costs include generic equipment for an AWE system, a downscaled floating platform, a mooring system, and transmission cables. Additionally, the commissioning costs for a generic airborne wind farm are included in this section.

4.4.1. AWE System and Floating Substructure

The floating wind platform literature this thesis is based on, tested ten different installation strategies to discover the most economical choice. The researchers concluded that their evaluated 1D strategy was the best choice pricewise, involving inshore assembly with two component lifts. The installation cost estimates below involve a 2 MW AWE system with each downscaled platform concept, using the 1D strategy, even though an AWE system will likely require only one component lift in a real installation scenario. The 1E strategy, involving inshore installation with one component lift, was not utilized in this work since the 1D strategy was less expensive (26).

The total installation cost for an individual AWE system and a floating platform were downscaled by one fourth of the original estimates in Ref. (26) due to a smaller floating platform

accommodating the AWE system. Once AWE reaches commercialization, installation costs for a floating AWE system will likely be lower, but over-estimating installation costs is appropriate for an economic feasibility analysis on technology in early development stages. The installation cost for an individual AWE system combined with the TLB-B and TLB-X3 platforms both equal $257.2k. The installation costs for an AWE system combined with the Hywind, WindFloat, and SWAY platforms are $263.2k, $215.7k, and $219.4k. These costs are further represented in Table A-3 in Appendix A.

4.4.2. Mooring System

The installation costs of the mooring system involve the anchors and mooring lines for each individual floating AWE system. It is assumed that they will be installed using a pre-laid out process, allowing for a longer window of opportunity to account for weather setbacks (6). Alternatively, installation of the mooring system for a large-scale offshore wind farm requires various operations due to the large number of anchors being installed and can involve a more complex installation process. Logistics would improve if multiple mooring lines and airborne wind systems were connected to a single high-capacity anchor, but investigating this strategy is beyond the scope of this research. The total installation and commissioning costs per airborne wind system at a 50 m depth are $64.3k for TLB-B and TLB-X3 concepts, $55.9k for Hywind, $74.3k for WindFloat, and $ 29.5k for SWAY.

4.4.3. Grid Connection System

The installation costs for the grid connection system involves the inter-array and export cables. A substation is not included in the installation costs for this study, due to the benchmark wind farm existing 15 km offshore, making the addition of one unnecessary. Installation costs

per km of cable and total grid connection costs for each airborne wind farm concept were determined. The installation cost for the export cable is normally one third of the inter-array cable. The inter-array and export cable installation costs per km of cable are based on Ref. (26) and are $ 795.8k/km and $ 265.3k/km. The total installation costs of the inter-array and export cables for a utility-scale wind farm, 15 km from shore are estimated at *M*$11.9 and *M*$4.

4.5. Operation and Maintenance

The operation and maintenance costs of a generic airborne wind farm, close to shore are included in this section. The maintenance of an offshore wind farm can be divided into three categories including, calendar based preventive maintenance, condition-based preventive and planned corrective maintenance, and unplanned corrective maintenance (6). The calendar-based preventive maintenance involves fixed time intervals and operating hours for servicing and repair of the airborne wind turbines. The condition-based preventive and planned corrective maintenance only initiates service and repair efforts once the wear of a wind turbine has surpassed set limits. This type of maintenance also monitors the actual condition of the systems. The unplanned corrective maintenance only services and repairs a turbine after system failure. The sourced literature of this data was originally estimated for a windfarm 200 km from shore. Adjustments were applied to represent operation and maintenance costs for a wind farm closer to shore. The total operation and maintenance costs per year for a 500 MW offshore wind farm are represented in Table 11. The costs are broken down into three categories, including material costs, labor costs, and equipment costs to equal a total annual operation and maintenance cost of *M$*23.3. Additionally, the construction phase insurance is an important cost factor when calculating the OPEX and was estimated at $24k/year.

Table 11. Total operation and maintenance costs per year for a 500 MW offshore airborne wind farm.

Annual Operation and Maintenance	***Costs ($)***
Material costs	
Unplanned corrective	$ 1799k
Condition-based	$ 44k
Calendar-based	$ 536k
Labor costs	
Unplanned corrective and calendar-based	$ 6428k
Condition-based	$ 43k
Equipment costs	
Unplanned corrective and calendar-based	*M$* 14.4
Condition-based	$ 499k
Total costs of repair per year	***M$* 23.3**

4.6 Decommissioning and Disposal

The decommissioning and disposal of wind turbines occurs at the end of their functional life. This life cycle phase involves the removal of every wind farm component including the turbines, floating platforms, mooring systems, and cabling system. Most countries require a detailed plan for decommissioning and disposal before the approval of a wind farm occurs, during the consenting and development phase. The same technique for the decommissioning phase used in Ref. (26) is utilized in this section. The decommissioning of a generic 500 MW wind farm with conventional turbines takes approximately one year. A common practice involves cutting the cables at a specific water depth and leaving the remaining cable units buried under the seabed. All other components are removed and transported to shore to be recycled and used as scrap metal. It is common for these recycled materials to have residual value, but that is not investigated further in this work. The total decommissioning costs per MW and scrap revenue for each concept are represented in Table 12. The revenue potential from recycling scrap

metal is shown for the Hywind, WindFloat, and SWAY technologies, resulting in negative total cost values. The TLB-B and TLB-X3 concepts have positive total cost values, since these designs originally use less steel during the production phase compared to the other three concepts.

Table 12. Projected decommissioning costs per MW. All costs in ^{2019}.

Concept	***TLB-B***	***TLB-X3***	***Hywind***	***WindFloat***	***SWAY***
Decommissioning costs	$ 68.7k	$ 68.7k	$ 68k	$ 64.6k	$ 57k
Scrap revenue	$ 44.5k	$ 47.6k	$ 104.2k	$ 142k	$ 64.6k
Total costs ($)	**$ 24.2k**	**$ 21.1k**	**-$ 36.2k**	**-$ 77.4k**	**-$ 7.6k**

Chapter 5. Techno-Economic Analysis

5.1. Wind Resource Analysis

In this section, the analysis for harvesting operations, with varying height at a specific location in the Gulf of Mexico is discussed. ERA5-Reanalysis wind data was utilized for the wind profile and carried out in 1-hour intervals and examined for wind speed and optimal harvesting height throughout a 41-year period (1979-2019). The specific location investigated in the Gulf of Mexico is 15 km offshore from Venice, Louisiana. A fully functioning electrical transmission cable exists in Venice, making it an ideal port area for a proposed utility-scale airborne wind farm, to supply nearby New Orleans with renewably sourced electricity.

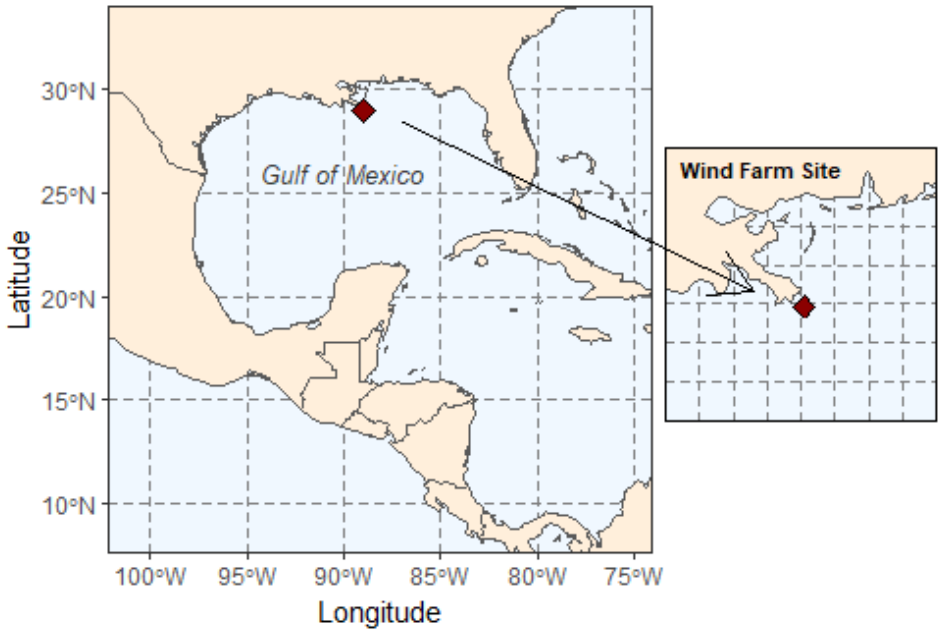

Figure 32. Hypothetical wind farm location at 28.95°N, -88.96°W, 15 km off the coast of Venice, Louisiana.

The following figures represent the wind data associated with this fictitious wind farm site. Due to insufficient wind speeds in the majority of the Gulf of Mexico at 90 m height, apart from Texas, offshore conventional windfarms have not been considered as a practical energy solution. Airborne windfarms are potentially ideal for locations such as the Gulf of Mexico, where wind harvesting takes places at a range of altitudes. The different harvesting heights and monthly average mean wind speeds at the hypothetical wind farm are shown in Figure 33.

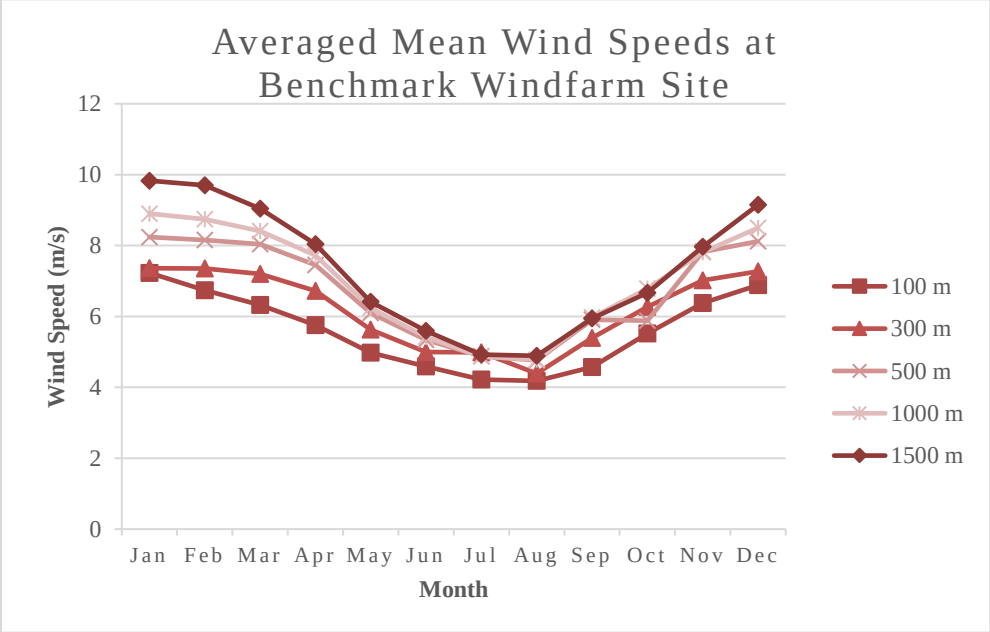

Figure 33. Comparison of averaged mean wind speeds at varying harvesting heights at location 28.95°N, -88.96°W in the Gulf of Mexico for January 1979 – December 2019.

The hourly interval wind speeds for each day were averaged together to yield mean wind speeds for each month at the benchmark wind farm site. The monthly averaged mean wind speeds were further averaged for the total 41-year period (1979-2019) to produce the results in Figure 33. The monthly averaged mean wind speeds were analyzed at different altitudes, which include the 100 m base case, and 300 m, 500 m, 1000 m, and 1500 m harvesting heights. Typically, an increase in wind speed is observed with increased altitude at most sites across the

world. At the studied test site, minor increases are observed with increased altitude. The wind speed is about 3 m/s greater at all harvesting heights during the winter months when compared to summer months. January has the highest averaged mean wind speed at 8.31 m/s between 100-1500 m heights. July and August have relatively similar wind speeds for all heights observed and have the lowest averaged mean wind speeds. The months of July and August have averaged mean wind speeds of 4.78 m/s and 4.60 m/s between 100-1500 m heights. Overall, the colder months of December, January, and February possess the highest averages for combined harvesting height, with marginal difference between each height during the warmest period of the year, specifically in July and August.

The monthly averaged mean wind speeds are further displayed in Figure 34. Dot plots were chosen to represent the wind resource for each month in offshore Louisiana. Even with certain months producing greater wind speeds, all show an increasing trendline, meaning wind speed increases with altitude for every month.

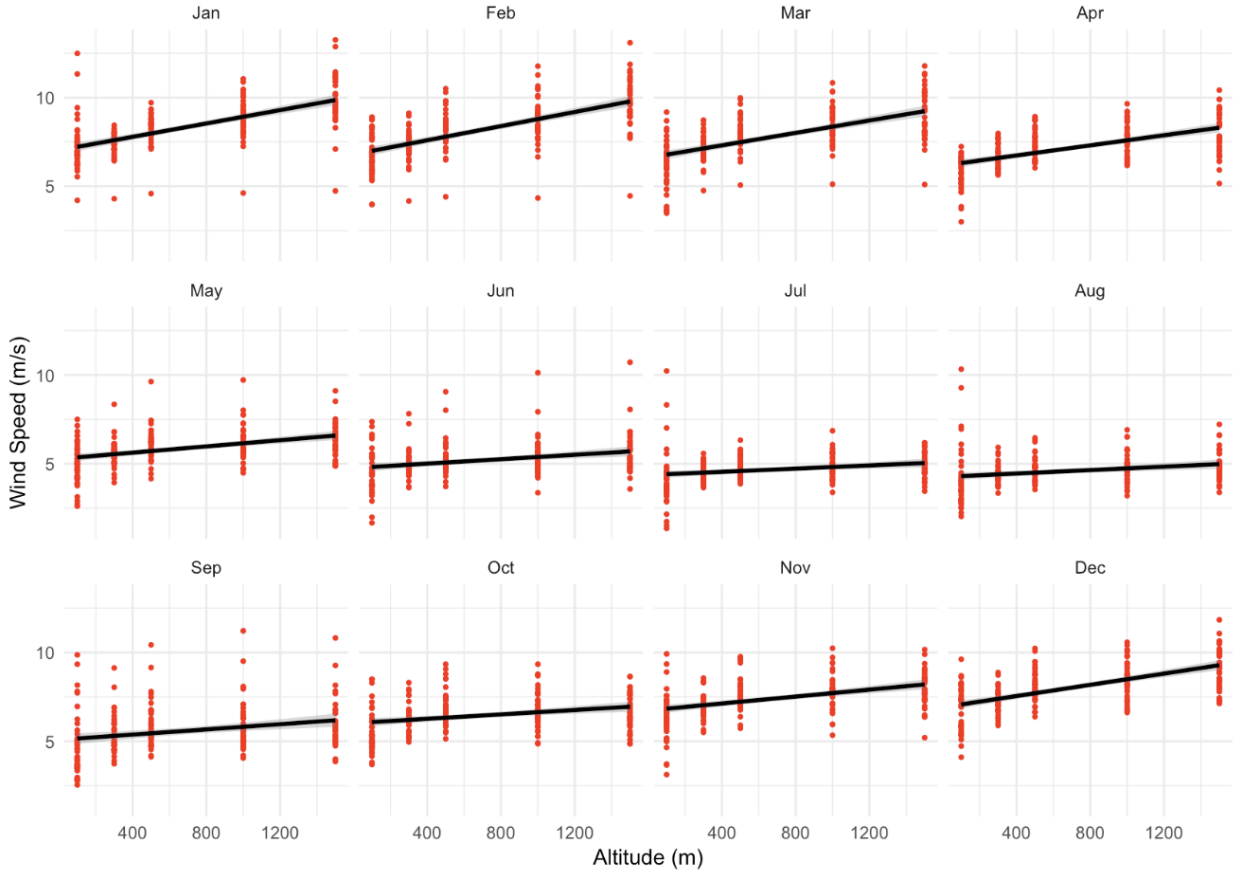

Figure 34. Averaged monthly mean wind speeds at 100 m, 300 m, 500 m, 1000 m, and 1500 m altitudes for January 1979-December 2019 at hypothetical wind farm site.

A Weibull distribution curve was constructed for combined harvesting heights (100-1500 m) to determine whether the tested site is ideal for offshore wind development. The two-parameter Weibull distribution function is a necessary tool used by the wind industry to understand the average power of measured wind data. The function incorporates a dimensionless shape factor (k), and scale parameter (c) expressed in m/s (16). Calculating the average mean wind speed is not an appropriate method when accurately representing wind power at a potential wind farm site. Without the use of the Weibull distribution method, wind resources would be underestimated. The Weibull distribution for combined harvesting heights (100-1500 m),

produced a scale factor that better represents the mean wind speed for the studied location, compared to the averaged mean wind speed results. Figure 35 represents the mean wind speed for combined harvesting heights using the Weibull distribution. The mean wind speed Weibull parameters are $c = 7.28$ m/s and $k = 3.91$ (corresponding average mean wind speed of 6.58 m/s). Generally, for a potential site to be ideal for offshore wind development, the mean wind speed needs to equal at least 7 m/s (34). Based on the 40-year mean wind speed Weibull parameters for 100-1500 m heights, the case study site is ideal to support wind farm development. These results do not fully represent the high-altitude wind resources for the entire Gulf of Mexico, but potentially represent wind resources at most offshore Louisiana locations 15 km from shore. Further studies on potential sites further offshore in the Gulf of Mexico should be conducted to determine the extent distance has on wind resources.

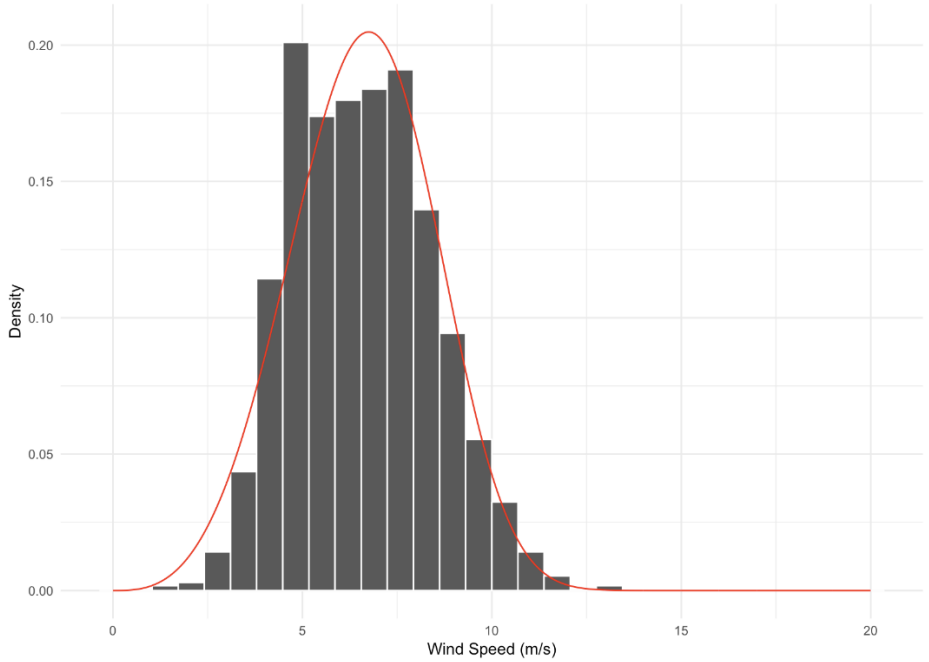

Figure 35. Density curve for wind resources between 100-1500 m heights from January 1979-December 2019. The mean wind speed Weibull parameters at combined harvesting heights, 15 km offshore of Venice, Louisiana are $c = 7.28$ m/s and $k = 3.91$ (corresponding average mean wind speed of 6.58 m/s).

The main advantage of installing an airborne windfarm over a conventional windfarm is that an AWE system can be easily adjusted to different altitudes. The Weibull distribution curves for a 40-year period at the case study site were created for each studied altitude level. The mean wind speed Weibull parameters at 100 m are $c = 6.23$ m/s and $k = 3.53$ (corresponding average mean wind speed of 5.61 m/s). The mean wind speed Weibull parameters are $c = 6.71$ m/s and $k = 5.41$ at 300 m, and $c = 7.44$ m/s and $k = 4.88$ at 500 m (corresponding average mean wind speeds of 6.22 m/s and 6.73 m/s). The mean wind speed Weibull parameters are c =7.69 m/s and $k = 4.36$ at 1000 m, and $c = 8.13$ m/s and $k = 3.86$ at 1500 m. (corresponding average mean wind speeds of 7.01 m/s and 7.35 m/s). These results indicate ideal harvesting heights exist above 500 m for offshore Louisiana (<15 km), since the Weibull mean wind speed is above 7 m/s. The average hub height for a conventional wind turbine is about 100 m, while the average harvesting height for an AWE system is 500 m. The density curves for the base case (100 m), and 500 m harvesting heights are represented in Figures 36 and 37. The density curves for the 300 m, 1000 m, and 1500 m heights are represented in Appendix B.

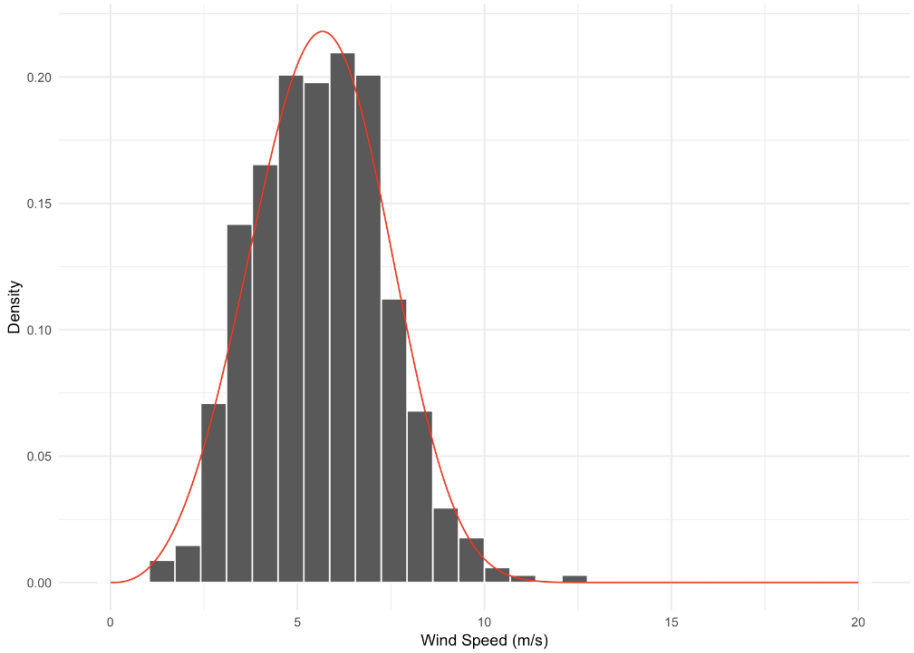

Figure 36. Density curve of wind resources for the average wind harvesting height of a conventional wind turbine (100 m), at the hypothetical wind farm, with mean wind speed Weibull parameters, $c = 6.23$ m/s and $k = 3.53$ (corresponding average mean wind speed of 5.61 m/s).

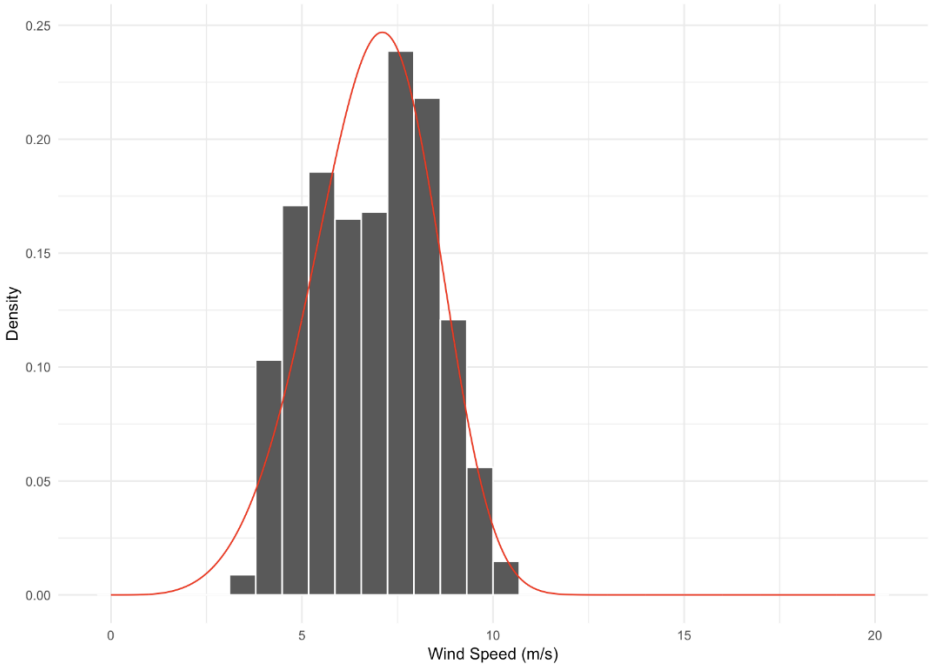

Figure 37. Density curve of wind resources for the average wind harvesting height of an AWE system (500 m), at hypothetical wind farm, with mean wind speed Weibull parameters, $c = 7.44$ m/s and $k = 4.88$ at 500 m (corresponding average mean wind speed of 6.73 m/s).

5.2. Economic Feasibility Cost Model

A net present value (NPV) model was conducted on each of the five windfarm concepts in this economic feasibility analysis section. The expected lifetime of this project is 30 years because the normal lifespan of a conventional wind turbine ranges between 20-30 years. The capital expenditures and operational expenditures are essential parameters to carry out an NPV cost model and were calculated from the LCCA in Chapter 4. The estimated capital expenditures, operational expenditures, and base case NPV cost model for each windfarm concept are discussed in the following sections.

5.2.1. Capital Expenditures

This section summarizes all baseline capital expenditures (CAPEX) from the LCCA in Chapter 4 and are represented in Table 13 for all floating windfarm concepts. The table shows that the 500 MW airborne windfarm with TLB-B platforms has the lowest CAPEX at the benchmark site, and the TLB-X3 wind farm has the second lowest total estimates. The WindFloat windfarm has a significantly higher CAPEX compared to all other concepts, due to the platform's weight and the substantial use of steel during production. The per MW CAPEX ($\$^{2019}$) calculated for each floating wind farm concept was utilized in the base case NPV cost model.

Table 13. Estimated capital expenditures (CAPEX) per MW.

CAPEX	***TLB-B***	***TLB-X3***	***Hywind***	***WindFloat***	***SWAY***
Developing and consenting	$ 279k	$ 279k	$ 279k	$ 279k	$ 279k
Construction phase insurance	$ 67k	$ 67k	$ 67k	$ 67k	$ 67k
Cost of AWE system (2 MW)	$ 118.6k	$ 118.6k	$ 118.6k	$ 118.6k	$ 118.6k
Production cost of platform	$ 133.5k	$ 171.2k	$ 534.3k	$ 1071.4k	$ 392.9k
Mooring costs (including installation)	$ 248.5k	$ 265.9k	$ 70.7k	$ 96k	$ 142.9k
Grid costs (including installation)	$ 60.9k	$ 60.9k	$ 60.9k	$ 60.9k	$ 60.9k
Installation of AWES and platform	$ 128.6k	$ 128.6k	$ 131.6k	$ 107.8k	$ 109.7k
Per MW CAPEX ($\$^{2019}$)	**$ 1036.1k**	**$ 1091.2k**	**$ 1262.1k**	**$ 1800.7k**	**$ 1171k**
Benchmark farm CAPEX (500 MW)	***M$* 518**	***M$* 545.6**	***M$* 631.1**	***M$* 900.4**	***M$* 585.5**

The CAPEX is visibly broken down in Figure 38, showing that the total production costs of the Hywind, WindFloat, and SWAY windfarms represents the largest portion of their total estimates. The overall lower CAPEX of the TLB-B and TLB-X3 windfarms is due to their much lower total production costs, which is a substantial advantage over the other concepts. The downside of both TLB windfarm concepts is that the production and installation of the mooring system is the most expensive aspect of their total CAPEX, while the other three concepts have much lower mooring system costs.

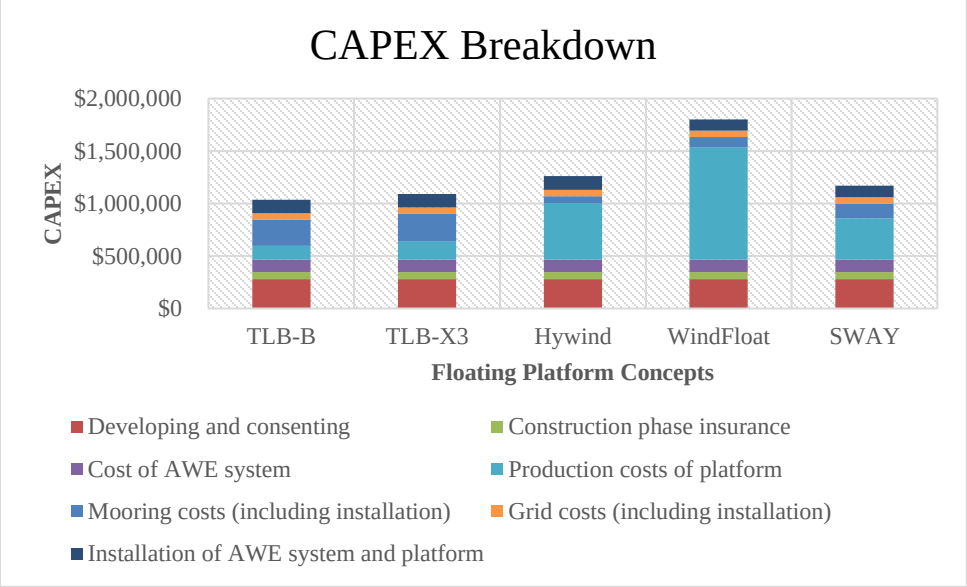

Figure 38. Visual representation of the different aspects incorporated into the total benchmark farm CAPEX for each 500 MW floating wind farm concept.

5.2.2. Operational Expenditures

This section summarizes all operational expenditures (OPEX), determined from the operation and maintenance costs and operational phase insurance costs in Chapter 4. The OPEX costs per MW ($\$^{2019}$/annum) and for a 500 MW benchmark farm are presented in Table 14. The same OPEX costs were applied for all five floating wind farm concepts in the base case NPV cost model carried out in the following section

Table 14. Estimated operational expenditures (OPEX) per MW.

Descriptions	***Cost ($)***
Annual operation and maintenance costs ($)	47.4k
Annual operational phase insurance costs ($)	24.1k
Per MW OPEX ($\$^{2019}$/annum)	71.5k
Benchmark farm OPEX	***M$* 35.8**

5.2.3. Base Case Study

The NPV base case was calculated for a 30-year period, assuming a discount rate of 4.5% [10]. The annual results for the base case NPVs of each windfarm concept are provided in Table 15. The base case NPVs for the TLB-B and TLB-X3 windfarms are *M$*293.7 and *M$*260.7, the Hywind wind farm is *M$*158.5, the WindFloat wind farm is *M$*-163.5, and the SWAY wind farm is *M$*213.6. The NPV is a good indicator of whether a potential project is worth an investment. A positive NPV value indicates a project is worth investing in, while a negative NPV value means the project is not worth investment. The TLB-B, TLB-X3, Hywind, and SWAY windfarm all produced a positive NPV suggesting that these four concepts will generate a return on investment (ROI) at base case cost estimates. Alternatively, the WindFloat windfarm produced a negative NPV, suggesting it will not generate an ROI. The detailed table for the entire 30-year NPV cost model for each wind farm concept is represented in the Table C-1 in Appendix C.

5.2.4. Break Even Analysis

A break-even analysis was completed for the WindFloat technology since it was the only floating platform wind farm to produce a negative base case NPV. Different parameters were altered to achieve a zero NPV. The adjusted parameters were the CAPEX, fixed OPEX, capacity factor, and discount rate. The comparison between the original base case parameters and the break-even values are represented in Table 15. The CAPEX was the first variable adjusted to produce a break-even cost of $1,526.59. The fixed OPEX needs to equal $48.14 to break-even. The capacity factor needs to be modified to 75.88% to reach the break-even cost. Lastly, a discount rate of 2.79% is necessary to break-even.

Table 15. Original base case parameters and break-even analysis for the WindFloat platform concept.

Parameters	***WindFloat Base Case***	***Break-Even Analysis***
CAPEX $(\$/kW)^{2019}$	$ 1,800.70	$ 1,526.59
Fixed OPEX $(\$/kW/yr)^{2019}$	$ 71.74	$ 48.14
Capacity factor (%)	68.00%	75.88%
Discount rate (%)	4.50%	2.79%

A break-even analysis was also conducted on four of the five platform concepts after increasing their original CAPEX values by 40% to reach a mature technology cost, which is further addressed in the sensitivity study. Only the TLB-X3, Hywind, WindFloat, and SWAY concepts were evaluated since the TLB-B concept still resulted in a positive NPV value after the mature technology adjustment. The tested variables were the fixed OPEX, capacity factor, and discount rate. The break-even cost for CAPEX remains $1,526.59 for all platform concepts, which is the same value calculated in the previous WindFloat base case analysis. The fixed OPEX, capacity factor, or discount rate for the TLB-X3 concept can be adjusted to $71.45, 68.03%, or 4.49% to break-even. The fixed OPEX, capacity factor, or discount rate for the Hywind concept can be altered to $51.03 or 74.91%, or 2.98% to break-even. Only the capacity factor for the WindFloat platform can be adjusted to 96.60% to reach the break-even cost, while the fixed OPEX and discount rate do not produce feasible results. Lastly, the fixed OPEX, capacity factor, or discount rate for the SWAY concept can be changed to $61.92, 71.24%, or 3.74% to break-even. Further representation of these results is in Table C-2 located in Appendix C.

5.3. Sensitivity Study

In this sensitivity study, different key cost drivers were altered, while other variables remained constant to determine how they changed the NPV base case costs for each wind farm concept. Different input variables were altered in this sensitivity study. The discount rate from 4.50% to 4.98%, which is based on the 2020 renewable energy cost of capital (12). Increasing the discount rate by this percentage produced a slight change in each concept, and the TLB-B, TLB-X3, Hywind, and SWAY remained positive, with WindFloat remaining as the only negative NPV. The mature technology costs for each wind farm were calculated by increasing the CAPEX by 40%. A significant change was observed, resulting in a negative NPV value for all concepts, except the TLB-B wind farm. The CAPEX and OPEX were then both increased by 40% and produced negative NPVs for all concepts. The base case electricity price was then increased and decreased by $0.01. Decreasing the electricity price by $0.01 resulted in positive NPV values for all concepts, while increasing it by $0.01 led to all negative NPVs. Additionally, the electricity production was analyzed by increasing and decreasing the base case capacity factor by 10%. Increasing the electricity production by 10% led to all positive NPVs, while decreasing it led to negative values only for the Hywind and WindFloat concepts. An overview of all adjusted cost factors and the resulting NPVs for each concept is represented in Table C-3 in Appendix C. All evaluated key cost drivers are discussed further in depth within the following sections.

5.3.1. Discount Rate

A more detailed NPV value was carried out for the discount rate to display the drastic impact that occurs when increased. The base case NPV previously carried out incorporated a

comparatively low discount rate of 4.5%, but in a real-world scenario the discount rate would most likely be greater. Changes in the discount rate took place at a range of intervals, which were 4%, 8%, 12%, 16%, 20%, and 24%. In Figure 39, NPV values considerably decrease when the discount rate is increased. By the time the discount rate reaches about 10% all wind farm concepts pass the break-even point and have negative NPV values. The discount rate cost estimates are further represented in Table C-4 in Appendix C.

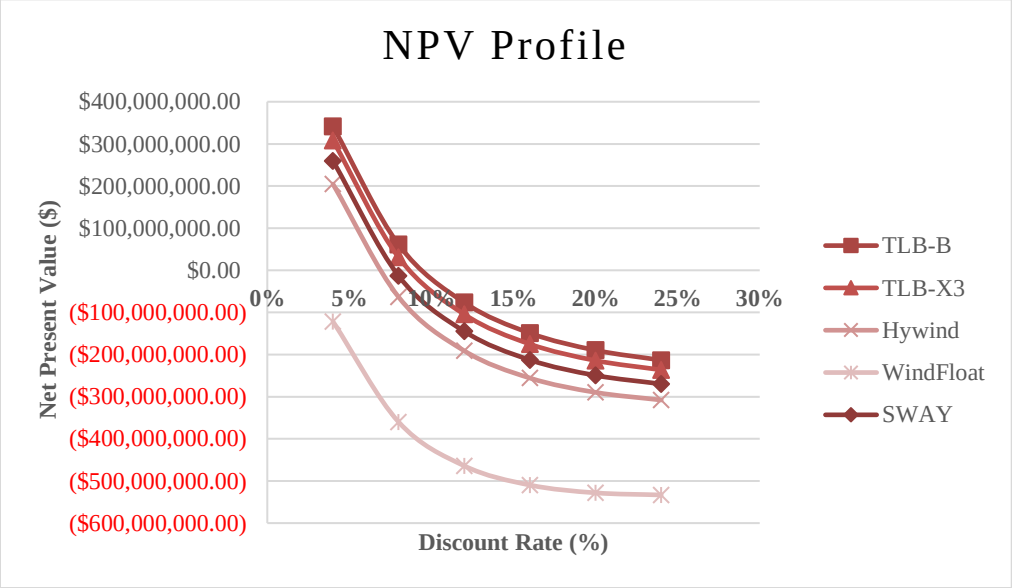

Figure 39. The NPV profile of each wind farm concept with increasing discount rates.

5.3.2. Mature Technology Cost

The CAPEX and OPEX used in the NPV base case study were increased by different percentages to determine the mature technology costs for each concept. Both cost factors were increased by 10%, 20%, 30%, and 40% and are represented in Figure 40. When an increase of 10% and 20% took place, the WindFloat concept was still the only resulting negative NPV. Increasing the CAPEX and OPEX by 30% resulted in a negative NPV for both the WindFloat and Hywind concepts. Lastly, a 40% increase was applied to all concepts, and resulted in

negative NPVs for all concepts, but TLB-B. The cost estimates for a 40% increase for TLB-B, TLB-X3, Hywind, WindFloat, and SWAY are *M$*45.9, *$*-278.1k, *M$*-143.3, *M$*-594.1, and *M$*-67.The mature technology cost, with a 40% increase of the CAPEX and OPEX base case for all concepts, was used as the final NPV cost estimates to determine investment potential for each airborne wind farm design on a commercial scale. The mature technology costs and other tested variables in this sensitivity study, indicate that the only airborne wind farm worth investing in at the studied test site is the TLB-B concept. The mature technology cost estimates are further represented in Table C-5 in Appendix C.

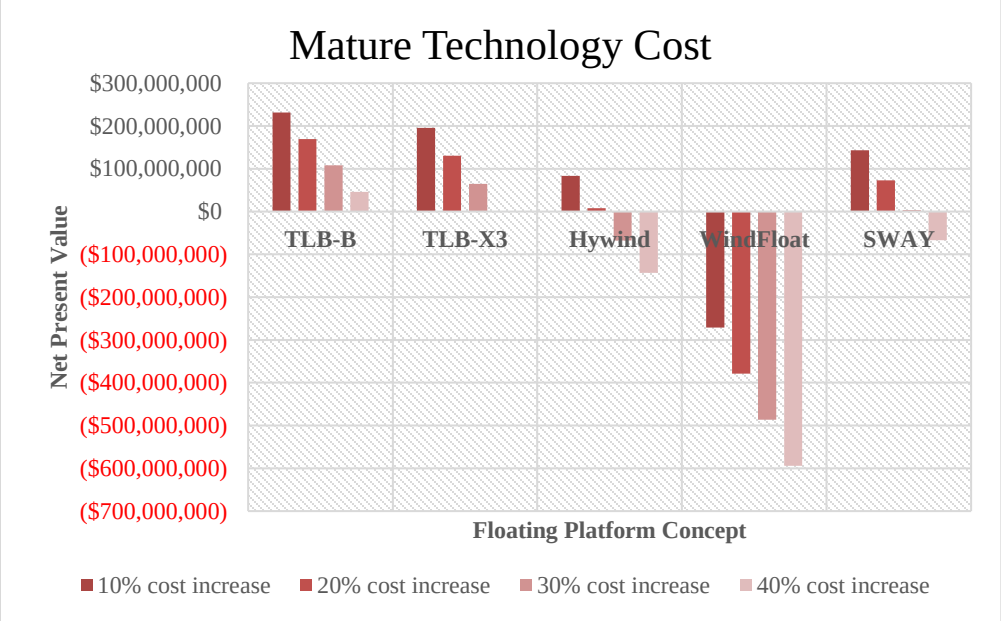

Figure 40. The mature technology costs for each wind farm concept.

5.3.3. Electricity Price

The electricity prices used in the base case NPV cost model were obtained from the EIA Annual Energy Outlook for 2019 and then decreased by $0.02, due to the novelty of airborne wind. The electricity price data used were from 2030-2060 to accurately represent a 30-year life

cycle of the hypothetical airborne wind farm. The average electricity base price of the data used equaled 3.35 cents per kilowatt an hour (kWh). The sensitivity analysis of electricity price represented in Figure 41 represents each wind farm concept when prices are decreased and increased by $0.01. Altering the electricity prices by one cent significantly influences whether a wind farm concept is profitable. When prices were increased by $0.01, all concepts had a positive NPV and far surpassed the break-even point. When prices were decreased by $0.01, all concepts produced a negative NPV. The sensitivity analysis of electricity price is further represented in Table C-6 in Appendix C.

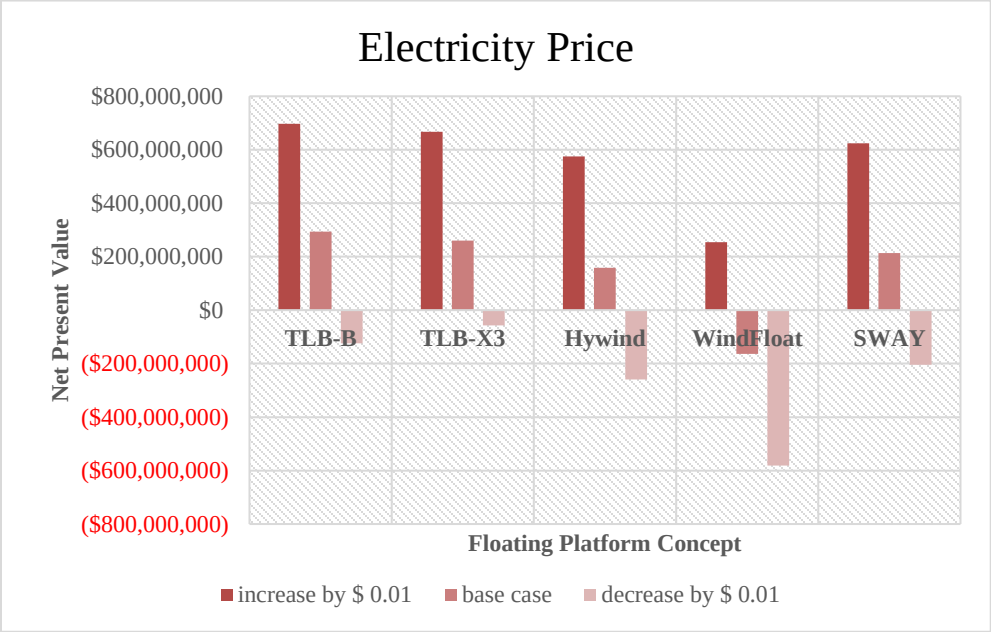

Figure 41. The NPVs of each wind farm concept when the electricity price variable is altered.

5.3.4. Electricity Production

The electricity production was altered to observe its impact on profitability and investment potential for each wind farm concept. The input variable present in the NPV cost model, representing electricity production is the capacity factor. A capacity factor of 68% was

used in the base case NPV model for all concepts. The capacity factor was increased by 10%, decreased by 10%, and decreased by 20% and are represented in Figure 42. When capacity factor was changed to 78%, all concepts produced a positive NPV. Decreasing the capacity factor to 58% resulted in negative NPVs for only the Hywind and WindFloat concepts. The capacity factor was then decreased further to 48%, which is roughly the capacity factor of conventional offshore wind, leading to negative NPVs for all concepts. This sensitivity study concludes that if capacity factor at a potential offshore site is 48% or lower, there is no investment potential for any floating airborne wind farm concept. The sensitivity analysis of electricity production is further represented in Table C-7 in Appendix C.

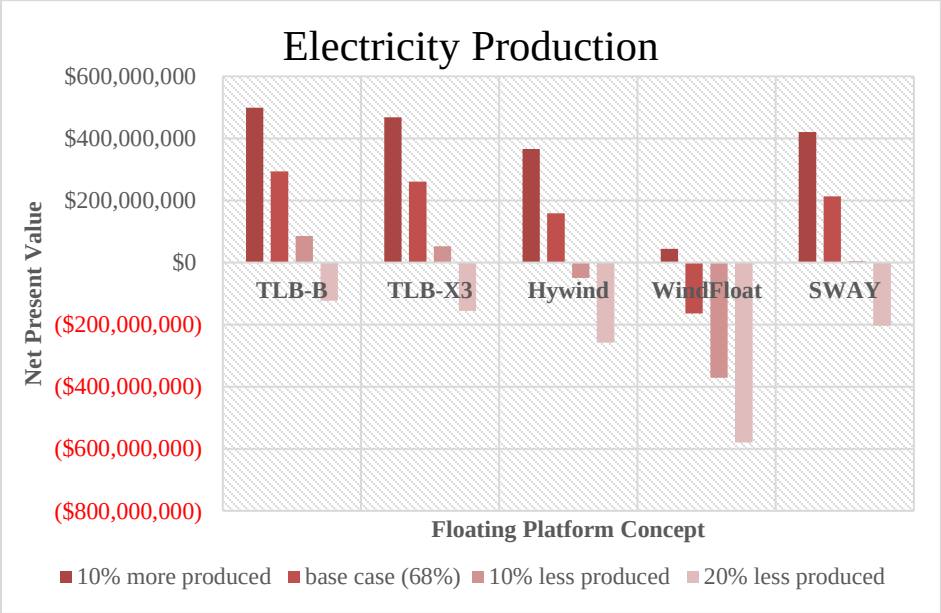

Figure 42. The sensitivity analysis of electricity production by altering the base case capacity factor in the NPV cost model.

Chapter 6. Conclusions

6.1. Primary Results and Conclusions

This thesis aimed to evaluate all necessary costs associated with the entire life cycle of five floating offshore airborne wind farm concepts. The costs related to different life phases including, development, construction, operation, and decommissioning were estimated. These costs were further evaluated in economic feasibility cost models, utilizing the net present value (NPV) method for each wind farm concept to determine their potential for project investment. A high-altitude wind resource analysis was conducted at a hypothetical wind farm site in the Gulf of Mexico, to investigate the wind resources at 100-1500 m harvesting heights. Sensitivity studies were carried out for each wind farm on key cost factors including, discount rate, CAPEX, OPEX, electricity price, and electricity production.

A hypothetical benchmark site was utilized for all five concepts, with a location 15 km offshore from Venice, Louisiana. General conditions were incorporated for each wind farm concept including, 50 m water depth, a generic pumping-kite 2 MW AWE system with a ground-based generator, and a total wind farm capacity of 500 MW. The proximity of the wind farm to shore and shallow water depth allowed for significantly lower OPEX and CAPEX estimates, compared to the original literature utilized for this work. The final NPVs calculated represent the mature technology costs of each wind farm concept.

The base case NPVs were adjusted to represent the mature technology costs by increasing the CAPEX by 40% for each concept. Based on mature technology values, only the TLB-B wind farm produced a positive NPV of *M$*45.9, indicating this platform technology incorporated with a 2 MW AWE system has investment potential on a utility-scale in the Gulf of Mexico,

specifically 15 km offshore. The one drawback to both TLB design concepts is their costly mooring system, potentially producing a negative NPV in water depths greater than 50 m. Alternatively, the costliest wind farm with the most notable NPVs for the base case and all sensitivity studies was the WindFloat concept. WindFloat was the only wind farm that produced a negative base case NPV. The sensitivity study on key cost factors conducted on this concept produced mostly negative NPVs. The significantly high production cost of the WindFloat concept is most likely due to the platform's high steel usage and substantial weight.

Even though a reference capacity factor of 68% was incorporated into the economic feasibility cost models, actual wind speeds were obtained 15 km offshore from Venice, Louisiana and analyzed for wind harvesting potential. The mean wind speed at the tested site was analyzed for 1-hour intervals over a 41-year period (1979-2019). An ideal site for offshore wind development needs to have a mean wind speed of at least 7 m/s. The Weibull mean wind speed for the combined wind harvesting heights (100-1500 m) at the hypothetical wind farm is 7.28 m/s, indicating the tested site is ideal for wind farm development, when accounting for all harvesting heights. The Weibull mean wind speeds at 100 m, 300 m, 500 m, 1000 m, and 1500 m heights are 6.23 m/s, 6.71 m/s, 7.44 m/s, 7.69 m/s, and 8.13 m/s. These results show that ideal wind resources exist above 500 m heights at the hypothetical wind farm.

Sensitivity studies were conducted on all concepts testing key cost factors. Adjusting the discount rate, CAPEX, OPEX, electricity price, and electricity production, led to a better understanding of how certain cost factors can produce positive NPVs. From these findings, it seems floating offshore airborne wind farms incorporating the TLB-B technology, may be competitive to conventional bottom-fixed and floating offshore wind farms closer to shore (<15

km offshore) and in shallow water depths (<50 m). The TLB-X3, Hywind, WindFloat, and SWAY concepts are not economically viable from a socioeconomic perspective in the Gulf of Mexico. However, through different support mechanisms such as tax incentives, floating offshore airborne wind energy for all concepts, at all distances from shore, and greater water depths could be economically reasonable in the Gulf of Mexico. Overall, these results clearly indicate the further necessity of cutting costs to ensure this new type of renewable energy is competitive with conventional wind systems, and other leading energy sources. The focus should be on decreasing the costs of the substructure component associated with each floating platform concept, the operation and maintenance costs, and grid connection costs, since these factors notably influence the levelized cost of energy.

6.2. Future Research

Further research is recommended in four main categories including the expansion and complexity of the techno-economic analysis, a multidimensional assessment, a feasibility analysis incorporating AWE systems with commissioned offshore oil and gas platforms, and economic potential of different floating wind platforms not addressed in this work.

Certain calculations including the capacity factor from the measured wind speed data at the hypothetical wind farm site and the levelized cost of energy (LCOE) should be computed. A reference capacity factor was utilized for all NPV cost models, due to time constraints and the complexity of calculating wind power for an AWE system. Research efforts are ongoing concerning accurate calculations of power curve and wind optimization estimates for airborne wind, which requires a more complex wind power formula, compared to conventional turbines. The LCOE would be the next calculation to further compare each wind farm concept and measures the lifetime costs divided by energy production. The LCOE is also considered the minimum constant price required to break-even over the lifetime of a project.

A multidimensional assessment evaluating other important aspects relating to offshore airborne wind development would be valuable. Specifically, research involving airspace safety of AWE systems and their environmental impacts, such as bird collisions are essential to future development of this technology in both onshore and offshore environments. Additionally, a further in-depth assessment on material choices for both AWE systems and floating platform concepts could lead to further cost-effective insights.

Investigating the feasibility of incorporating AWE systems on commissioned offshore oil and gas platforms would assist with commercialization efforts. Novel technology such as AWE

could benefit significantly from producing energy for off-grid locations, such as offshore oil and gas facilities. AWE concepts providing energy to offshore oil and gas platforms could be an excellent first step in commercialization before reaching utility-scale production.

Only five floating platform concepts were included in this work, but many others exist. Research incorporating newer floating platform technology with AWE systems could have greater investment potential estimates compared to most platforms analyzed in this research. Specifically, research on the SpiderFLOAT platform and its incorporation with AWE systems could lead to interesting insights, since it can potentially surpass all other existing design concepts.

Appendix A. Life Cycle Cost Assessment Tables

Table A-1. Total mooring system costs per floating airborne wind system at 50 m benchmark depth.

Concept	*Total Mooring System Cost ($)*
TLB-B	$ 432.6k
TLB-X3	$ 467.6k
Hywind	$ 85.5k
WindFloat	$ 117.6k
SWAY	$ 258.3k

Table A-2. Inter-array cable and export cable production costs per km and total cable costs for a benchmark wind farm, deployed 15 km offshore.

	Inter-array Cable	*Export Cable*
Costs ($/per km of cable)	$ 376.4k	$ 593.4k
Total grid connection costs for wind farm ($)	M$ 5.7	M$ 8.9

Table A-3. Estimated installation costs per AWE system for each floating platform concept.

Concept	*Installation Costs ($)*
TLB-B/TLB-X3	$ 257.2k
Hywind	$ 263.2k
WindFloat	$ 215.7k
SWAY	$ 219.4k

Table A-4. Total installation and commissioning costs of mooring systems per AWE turbine for each concept.

Concept	*Total Installation Cost per AWE System ($)*
TLB-B/TLB-X3	$ 64.3k
Hywind	$ 55.9k
WindFloat	$ 74.3k
SWAY	$ 29.5k

Table A-5. Installation costs for each grid system component per km.

Grid System Component	*Installation Costs per km ($)*
Inter-Array Cable	$ 795.8k
Export Cable	$ 265.3k

Table A-6. Total installation costs for a hypothetical wind farm existing 15 km offshore.

Grid System Component	*Total Installation Costs for 500 MW Wind Farm ($)*
Inter-Array Cable	M$ 11.9
Export Cable	M$ 4.0

Appendix B. Wind Resource Analysis Weibull Distributions

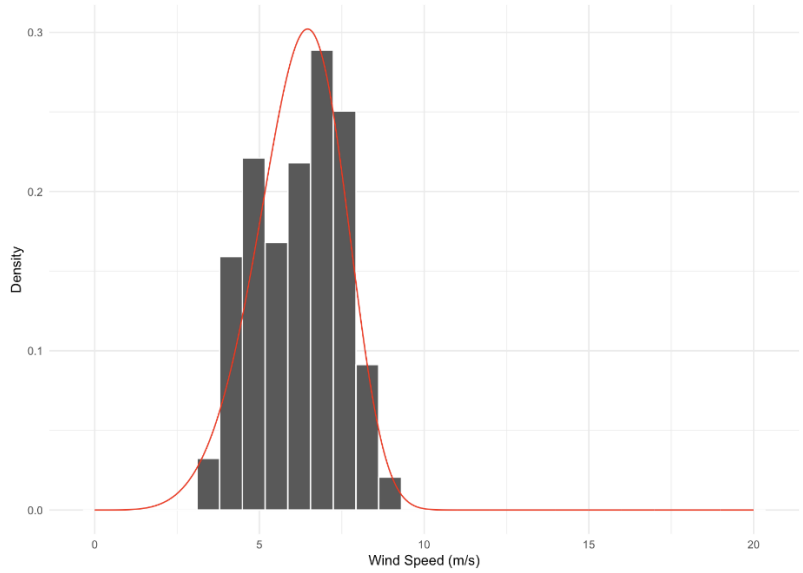

Figure B-1. Density curve of wind resources at 300 m height at hypothetical wind farm site, over a 41-year period, with a yearly mean wind speed of 6.71 m/s (1979-2019).

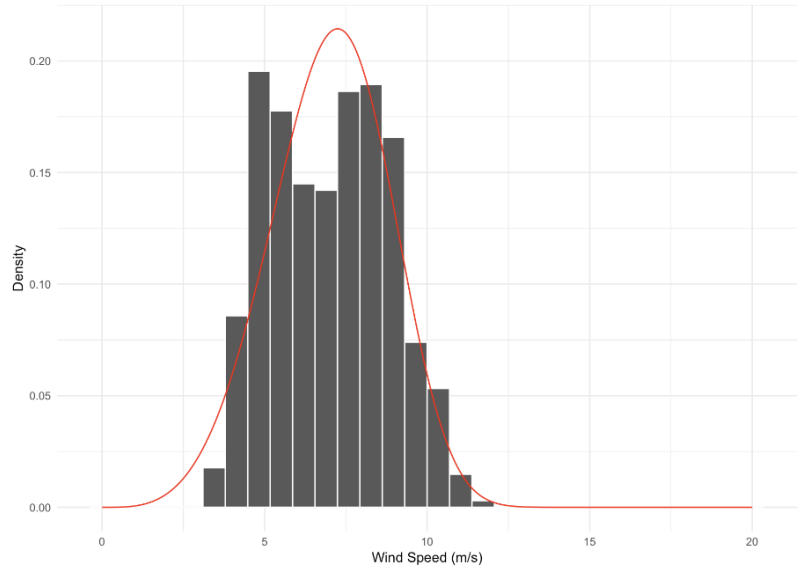

Figure B-2. Density curve of wind resources at 1000 m height at hypothetical wind farm site, over a 41-year period (1979-2019), with a yearly mean wind speed of 7.69 m/s.

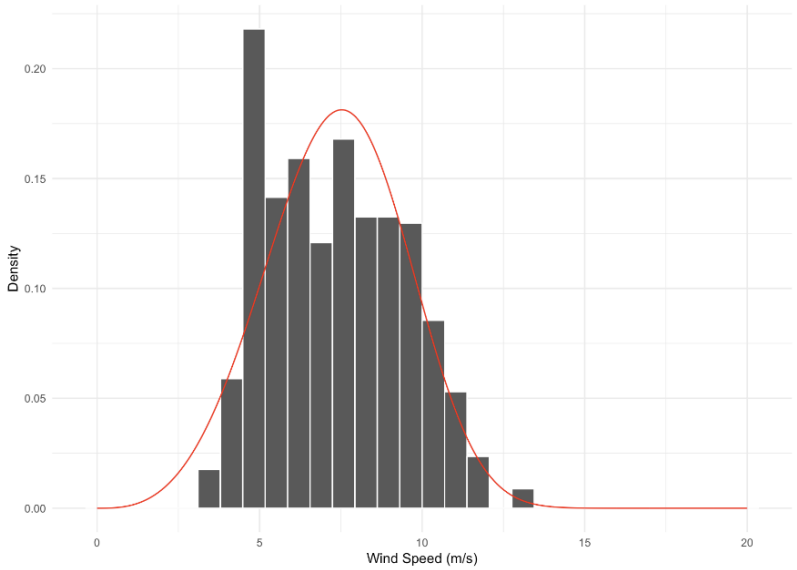

Figure B-3. Density curve of wind resources at 1500 m height at hypothetical wind farm site, over a 41-year period (1979-2019), with a yearly wind speed of 8.13 m/s.

Appendix C. Sensitivity Study Tables

Table C-1. The 30-year base case NPVs ($) for a 500 MW floating offshore airborne windfarm, with each floating platform concept.

Year	*TLB-B*	*TLB-X3*	*Hywind*	*WindFloat*	*SWAY*
0	*M$* -129.5	*M$* -136.4	*M$* -157.8	*M$* -225.1	*M$* -146.4
1	*M$* -153.9	*M$* -162.1	*M$* -187.5	*M$* -267.5	*M$* -173.9
2	*M$* -84.5	*M$* -92.4	*M$* -116.7	*M$* -193.2	*M$* -103.7
3	*M$* 32.6	*M$* 31.1	*M$* 26.6	*M$* 12.3	*M$* 29.0
4	*M$* 31.2	*M$* 29.8	*M$* 25.4	*M$* 11.8	*M$* 27.8
5	*M$* 29.8	*M$* 28.5	*M$* 24.4	*M$* 11.3	*M$* 26.6
6	*M$* 28.5	*M$* 27.3	*M$* 23.3	*M$* 10.8	*M$* 25.4
7	*M$* 27.3	*M$* 26.1	*M$* 22.3	*M$* 10.3	*M$* 24.3
8	*M$* 26.1	*M$* 25.0	*M$* 21.3	*M$* 9.9	*M$* 23.3
9	*M$* 17.1	*M$* 16.1	*M$* 12.7	*M$* 1.8	*M$* 14.5
10	*M$* 16.4	*M$* 15.3	*M$* 12.0	*M$* 1.6	*M$* 13.8
11	*M$* 34.9	*M$* 34.9	*M$* 34.9	*M$* 34.9	*M$* 34.9
12	*M$* 31.9	*M$* 31.9	*M$* 31.9	*M$* 31.9	*M$* 31.9
13	*M$* 30.5	*M$* 30.5	*M$* 30.5	*M$* 30.5	*M$* 30.5
14	*M$* 29.2	*M$* 29.2	*M$* 29.2	*M$* 29.2	*M$* 29.2
15	*M$* 27.9	*M$* 27.9	*M$* 27.9	*M$* 27.9	*M$* 27.9
16	*M$* 26.7	*M$* 26.7	*M$* 26.7	*M$* 26.7	*M$* 26.7
17	*M$* 25.6	*M$* 25.6	*M$* 25.6	*M$* 25.6	*M$* 25.6
18	*M$* 25.6	*M$* 25.6	*M$* 25.6	*M$* 25.6	*M$* 25.6
19	*M$* 24.5	*M$* 24.5	*M$* 24.5	*M$* 24.5	*M$* 24.5
20	*M$* 23.5	*M$* 23.5	*M$* 23.5	*M$* 23.5	*M$* 23.5
21	*M$* 21.6	*M$* 21.6	*M$* 21.6	*M$* 21.6	*M$* 21.6
22	*M$* 20.5	*M$* 20.5	*M$* 20.5	*M$* 20.5	*M$* 20.5
23	*M$* 19.4	*M$* 19.4	*M$* 19.4	*M$* 19.4	*M$* 19.4
24	*M$* 18.4	*M$* 18.4	*M$* 18.4	*M$* 18.4	*M$* 18.4
25	*M$* 17.5	*M$* 17.4	*M$* 17.5	*M$* 17.5	*M$* 17.5
26	*M$* 16.6	*M$* 17.5	*M$* 16.6	*M$* 16.6	*M$* 16.6
27	*M$* 15.7	*M$* 16.6	*M$* 15.7	*M$* 15.7	*M$* 15.7
28	*M$* 14.9	*M$* 15.7	*M$* 14.9	*M$* 14.9	*M$* 14.9
29	*M$* 14.2	*M$* 14.9	*M$* 14.2	*M$* 14.2	*M$* 14.2
30	*M$* 13.5	*M$* 14.2	*M$* 13.5	*M$* 13.5	*M$* 13.5
NPV Total	***M$* 293.7**	***M$* 13.5**	***M$* 158.5**	***M$* -163.5**	***M$* 213.0**

Table C-2. Break-even analysis of TLB-X3, Hywind, WindFloat, and SWAY floating wind farms with mature technology cost by adjusting CAPEX, fixed OPEX, capacity factor, and discount rate.

Parameters	***TLB-X3***	***Hywind***	***WindFloat***	***SWAY***
Fixed OPEX	$ 71.45	$ 51.03	$ -13.34	$ 61.92
Capacity Factor	68.03%	74.91%	96.60%	71.24%
Discount Rate	4.49%	2.98%	-0.20%	3.74%

Table C-3. Sensitivity study of a 30-year NPV ($) for a hypothetical 500 MW offshore floating airborne wind farm in the Gulf of Mexico of all five design concepts.

Assumption	*TLB-B*	*TLB-X3*	*Hywind*	*WindFloat*	*SWAY*
Original assumptions	M$ 293.7	M$ 260.7	M$ 158.5	M$ -163.5	M$ 213.6
Discount rate is 4.98% [10]	M$ 252.0	M$ 219.4	M$ 118.4	M$ -199.8	M$ 172.3
CAPEX increased by 40%	M$ 45.9	M$ -278.1	M$ -143.3	M$ -594.1	M$ -67.0
CAPEX and OPEX increased by 40%	M$ -154.6	M$ -200.7	M$ -343.8	M$ -794.6	M$ -267.4
Electricity prices increase by $ 0.01	M$ 697.1	M$ 667.4	M$ 574.9	M$ 253.9	M$ 624.5
Electricity prices decrease by $ 0.01	M$ -123.7	M$ -56.7	M$ -258.9	M$ -580.9	M$ -204.4
10% more electricity is produced	M$ 498.8	M$ 468.2	M$ 366.5	M$ 44.5	M$ 421.0
10% less electricity is produced	M$ 85.9	M$ 52.7	M$ -49.5	M$ -371.5	M$ 5.0
20% less electricity is produced	M$ -122.3	M$ -155.3	M$ -257.5	M$ -579.5	M$ -202.9

Table C-4. Discount rate based on 2020 green and renewable energy cost of capital.

Discount Rate	*TLB-B*	*TLB-X3*	*Hywind*	*WindFloat*	*SWAY*
4.98%	M$ 252.0	M$ 219.4	M$ 118.4	M$ -200	M$ 172.3

Table C-5. Estimated mature technology costs, with CAPEX and OPEX percentile increases.

CAPEX and OPEX	*TLB-B*	*TLB-X3*	*Hywind*	*WindFloat*	*SWAY*
10% Cost Increase	M$ 231.7	M$ 195.4	M$ 83.1	M$ -271.2	M$ 143
20% Cost Increase	M$ 169.8	M$ 130.2	M$ 7.6	M$ -378.8	M$ 73.0
30% Cost Increase	M$ 107.8	M$ 65.0	M$ -67.8	M$ -486.5	M$ 3.0
40% Cost Increase	M$ 45.9	$ -278.1k	M$ -143.3	M$ -594.1	M$ -67.0

Table C-6. Sensitivity analysis of electricity price fluctuations.

Electricity Price	*TLB-B*	*TLB-X3*	*Hywind*	*WindFloat*	*SWAY*
Increase by $ 0.01	M$ 697.1	M$ 667.4	M$ 574.9	M$ 253.9	M$ 624.5
Decrease by $ 0.01	M$ -123.7	M$ -56.7	M$ -258.9	M$ -580.9	M$ -204.4

Table C-7. Sensitivity analysis of electricity production through modifying capacity factor.

Electricity Production	***TLB-B***	***TLB-X3***	***Hywind***	***WindFloat***	***SWAY***
10% more produced	M$ 498.8	M$ 468.2	M$ 366.5	M$ 44.5	M$ 421.0
10% less produced	M$ 85.9	M$ 52.7	M$ -49.5	M$ -371.5	M$ 5.0
20% less produced	M$ -122.2	M$ -155.3	M$ -257.0	M$ -579.5	M$ -202.9

Table C-8. Sensitivity analysis incorporating a Production Tax Credit (PTC) incentive.

PTC Incentive	***TLB-B***	***TLB-X3***	***Hywind***	***WindFloat***	***SWAY***
$ 0.02	B$ 1.1	B$ 1.1	M$ 969.9	M$ 671.2	B$ 1.0

References

1. Ampyx Power. (2020). *Technology Explained.* Retrieved February 29, 2020, from https://www.ampyxpower.com/our-technology/

2. Ampyx Power, Energy Research Center Netherlands, Maritime Research Institute Netherlands, Mocean Offshore (2018). *Sea-Farm-Air Project: Demonstrating the potential of far offshore floating airborne wind farms, 2018.* Retrieved from https://energeia-binary-external prod.imgix.net/R4LFsRy4GrrRzYuw3LJjdTV5XL4.pdf?dl=The+Sea-Air-Farm+Project.pdf

3. Archer, C.L., *An introduction to meteorology for airborne wind energy*, in *Airborne wind energy*. 2013, Springer. p. 81-94.

4. Archer, C. L., Delle Monache, L., & Rife, D. L. (2014). Airborne wind energy: Optimal locations and variability. *Renewable Energy*, *64*, 180-186.

5. Bechtle, P., et al., *Airborne wind energy resource analysis.* Renewable energy, 2019. 141: p. 1103-1116.

6. Bjerkseter, C. and A. Ågotnes, *Levelised costs of energy for offshore floating wind turbine concepts*. 2013, Norwegian University of Life Sciences, Ås.

7. Borgonovo, E., & Peccati, L. (2004). Sensitivity analysis in investment project evaluation. *International Journal of Production Economics*, *90*(1), 17-25.

8. Bureau of Labor Statistics., *Archived News Releases | Producer Price Index.* (2020, April 10). Retrieved May 1, 2019, from https://www.bls.gov/bls/news-release/ppi.htm#2019

9. Cherubini, A., et al., *Airborne Wind Energy Systems: A review of the technologies.* Renewable and Sustainable Energy Reviews, 2015. 51: p. 1461-1476.

10. Cherubini, A., Vertechy, R., & Fontana, M. (2016). Simplified model of offshore airborne wind energy converters. *Renewable Energy*, *88*, 465-473.

11. Copernicus Climate Change Service (C3S) (2020): ERA5: Fifth generation of ECMWF atmospheric reanalyses of the global climate . Copernicus Climate Change Service Climate Data Store (CDS), *date of access*. https://cds.climate.copernicus.eu/cdsapp#!/home

12. Damodaran, A. (2020). History & Philosophy. Retrieved April 19, 2020, from http://pages.stern.nyu.edu/~adamodar/New_Home_Page/datahistory.html

13. Davis, R. A. (2017). Sediments of the Gulf of Mexico. In *Habitats and Biota of the Gulf of Mexico: Before the Deepwater Horizon Oil Spill* (pp. 165-215). Springer, New York, NY.

14. Faggiani, P. and R. Schmehl, *Design and economics of a pumping kite wind park*, in *Airborne Wind Energy*. 2018, Springer. p. 391-411.

15. Fleten, S. E., Linnerud, K., Molnár, P., & Nygaard, M. T. (2016). Green electricity investment timing in practice: Real options or net present value?. *Energy*, *116*, 498-506.

16. Genc, A., Erisoglu, M., Pekgor, A., Oturanc, G., Hepbasli, A., & Ulgen, K. (2005). Estimation of wind power potential using Weibull distribution. *Energy Sources*, *27*(9), 809-822.

17. González, J. S., Payán, M. B., & Santos, J. R. (2013). Optimum design of transmissions systems for offshore wind farms including decision making under risk. *Renewable energy*, *59*, 115-127.

18. Hywind. (2020). *Floating offshore wind in Equinor*, Retrieved February 29, 2020, from https://www.equinor.com/en/what-we-do/floating-wind.html.

19. Kaiser, M.J. and B. Snyder, *Offshore wind capital cost estimation in the US Outer Continental Shelf—A reference class approach.* Marine Policy, 2012. 36(5): p. 1112-1122.

20. Licitra, G., Koenemann, J., Bürger, A., Williams, P., Ruiterkamp, R., & Diehl, M. (2019). Performance assessment of a rigid wing Airborne Wind Energy pumping system. *Energy*, *173*, 569-585.

21. Mahmood, F. H., Resen, A. K., & Khamees, A. B. (2019). Wind characteristic analysis based on Weibull distribution of Al-Salman site, Iraq. *Energy Reports*.

22. Maienza, C., Avossa, A. M., Ricciardelli, F., Coiro, D., Troise, G., & Georgakis, C. T. (2020). A life cycle cost model for floating offshore wind farms. *Applied Energy*, *266*, 114716.

23. Makani Air. (2020). *Technology*. Retreived February 29, 2020, from https://makanipower.com/technology/

24. Malz, E. C., Hedenus, F., Göransson, L., Verendel, V., & Gros, S. (2020). Drag-mode airborne wind energy vs. wind turbines: An analysis of power production, variability and geography. *Energy*, *193*, 116765.

25. Musial, W., Butterfield, S., & Boone, A. (2004, January). Feasibility of floating platform systems for wind turbines. In *42nd AIAA aerospace sciences meeting and exhibit* (p. 1007).

26. Myhr, A., Bjerkseter, C., Ågotnes, A., & Nygaard, T. A. (2014). Levelised cost of energy for offshore floating wind turbines in a life cycle perspective. *Renewable energy*, *66*, 714-728.

27. Myhr, A. and T.A. Nygaard. *Load reductions and optimizations on tension-leg-buoy offshore wind turbine platforms*. in *The Twenty-second International Offshore and Polar Engineering Conference*. 2012. International Society of Offshore and Polar Engineers.

28. Myhr, A. and T.A. Nygaard, *Comparison of experimental results and computations for tension-leg-buoy offshore wind turbines.* 2015.

29. Pantusa, D. and G. Tomasicchio, *Large-scale offshore wind production in the Mediterranean Sea.* Cogent Engineering, 2019. 6(1): p. 1661112.

30. Ranneberg, M., Wölfle, D., Bormann, A., Rohde, P., Breipohl, F., & Bastigkeit, I. (2018). Fast power curve and yield estimation of pumping airborne wind energy systems. In *Airborne Wind Energy* (pp. 623-641). Springer, Singapore.

31. Roddier, D., et al., *WindFloat: A floating foundation for offshore wind turbines.* Journal of renewable and sustainable energy, 2010. **2**(3): p. 033104.

32. Roque, L. A., Paiva, L. T., Fernandes, M. C., Fontes, D. B., & Fontes, F. A. (2020). Layout optimization of an airborne wind energy farm for maximum power generation. *Energy Reports*, *6*, 165-171.

33. Ross, S.A., *Uses, abuses, and alternatives to the net-present-value rule.* Financial management, 1995. 24(3): p. 96-102.

34. Schwartz, M., et al. (2010). U.S. Offshore 90-Meter Wind Resource Potential. Retrieved April 23, 2020, from https://windexchange.energy.gov/maps-data/320

35. SkySails (2020). *Technology.* Retrived February 29, 2020, from: https://skysails-power.com/technology.html

36. SWAY, 2020. [cited 2020 29 February]; Available from: http://www.inocean.no/projects/sway-offshore-wind-turbine/.

37. Uzunoglu, E., Karmakar, D., & Soares, C. G. (2016). Floating offshore wind platforms. In *Floating Offshore Wind Farms* (pp. 53-76). Springer, Cham.

38. van der Vlugt, R., Peschel, J., & Schmehl, R. (2013). Design and experimental characterization of a pumping kite power system. In *Airborne wind energy* (pp. 403-425). Springer, Berlin, Heidelberg.

39. Waris, M. B., & Ishihara, T. (2012). Dynamic response analysis of floating offshore wind turbine with different types of heave plates and mooring systems by using a fully nonlinear model. *Coupled systems mechanics*, *1*(3), 247-268.

40. WindFloat. (2020). *Technology.* Retrieved February 29, 2020, from http://www.principlepowerinc.com/en/windfloat.

41. Zore, Ž., et al., *Maximizing the sustainability net present value of renewable energy supply networks.* Chemical Engineering Research and Design, 2018. 131: p. 245-265.

Vita

Alexandria Savannah Leake, born in Marietta, Georgia, attended Louisiana State University for her undergraduate degree and received her bachelor's in coastal environmental science in May of 2018. She was offered a graduate assistantship as the recruiter for the CES undergraduate program at LSU after graduation. She decided to enter the Department of Environmental Sciences and has worked as the CES recruiter while completing graduate school coursework and thesis research throughout the past two years. Her interest in renewable energy continued to grow throughout graduate school and she would like to eventually work for the Department of Energy or an energy related company in the private sector. Upon completion of her master's degree, she will be moving back home to Atlanta, Georgia to help open her family's brewery, High Shoals, and will train to become a beer brewing master.